Heavy-Ion Double Charge Exchange reactions towards $0\nu\beta\beta$ NME determination : the NUMEN project

Clementina Agodi

for

the NUMEN collaboration

SPES one-day Workshop " Probing fundamental symmetries and interactions by low energy excitations with SPES RIBs"

1-2 February 2018 - *INFN, Pisa*

Outline

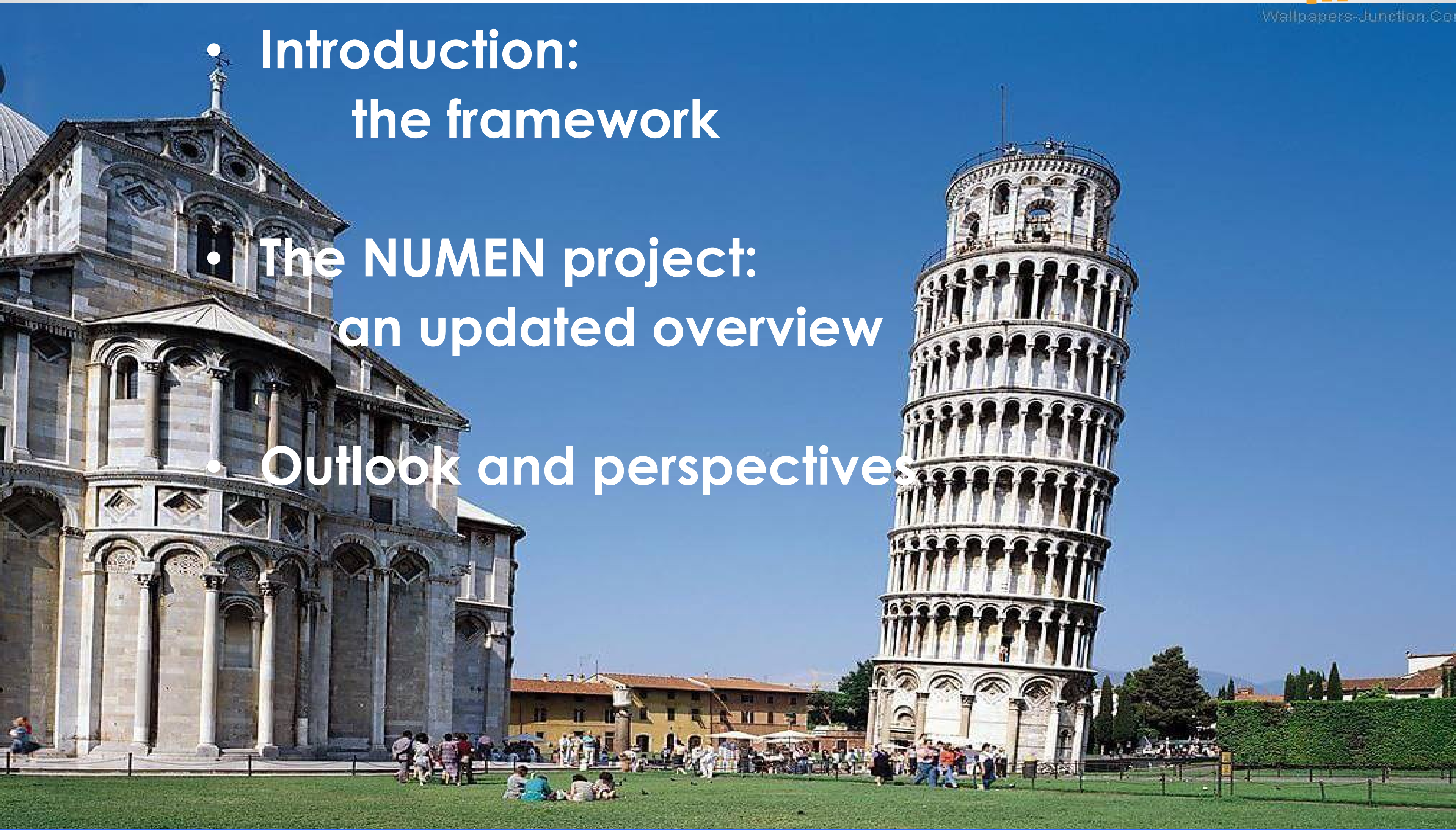

- Introduction:
  the framework
- The NUMEN project:
  an updated overview
- Outlook and perspectives

Introduction

Unanswered questions in neutrino physics:

- What is the absolute mass scale of neutrinos?

  E. Fermi, Z. Phys. 88, 161

  ... 14, 171 (1937)

  ... neutrino species are there?

  B. Pontecorvo, Sov. Phys. JETP 26, 984 (1968)

An answer to all three questions can be obtained from neutrinoless double-beta decay (DBD) and related processes

Indeed, if observed, neutrinoless DBD may provide evidence for physics beyond the Standard Model other than the mass mechanism.

Conversely, its non-observation will set stringent limits on other scenarios (sterile,…), and on non standard mechanisms

Neutrinoless double beta decay

$$ {}^{A}_{Z}X_{N} \rightarrow {}^{A}_{Z+2}Y_{N-2} + 2e^{-} $$

Still not observed

1. **Beyond standard model**
2. **Access to effective neutrino mass**
3. **Violation of lepton number conservation**
4. **CP violation in lepton sector**
5. **A way to leptogenesis and GUT**

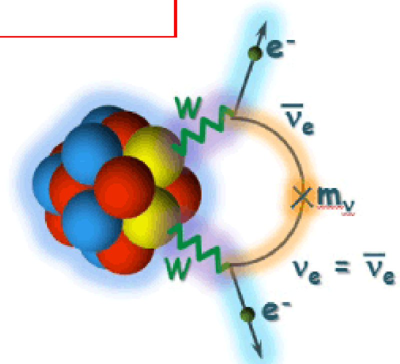

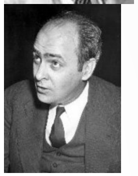

E. Majorana, Il Nuovo Cimento 14 (1937) 171
W. H. Furry, Phys Rev. 56 (1939) 1184

$$ \left[\tau_{1/2}^{0\nu\beta\beta}(0^{+} \rightarrow 0^{+})\right]^{-1} = G_{0\nu}\left|M_{0\nu}\right|^{2}\left|f(m_i, U_{ei})\right|^{2} $$

Phase-space factor
(Atomic physics)
PSF

Matrix elements
(Nuclear physics)
NME

Beyond the standard model
(Particle physics)

Nuclear matrix elements

$$\left|M_{\varepsilon}^{\beta\beta 0\nu}\right|^2 = \left|\left\langle 0_f \left\| \hat{O}_{\varepsilon}^{\beta\beta 0\nu} \right\| 0_i \right\rangle\right|^2$$

Comparison of the main NME calculations: spread about x2

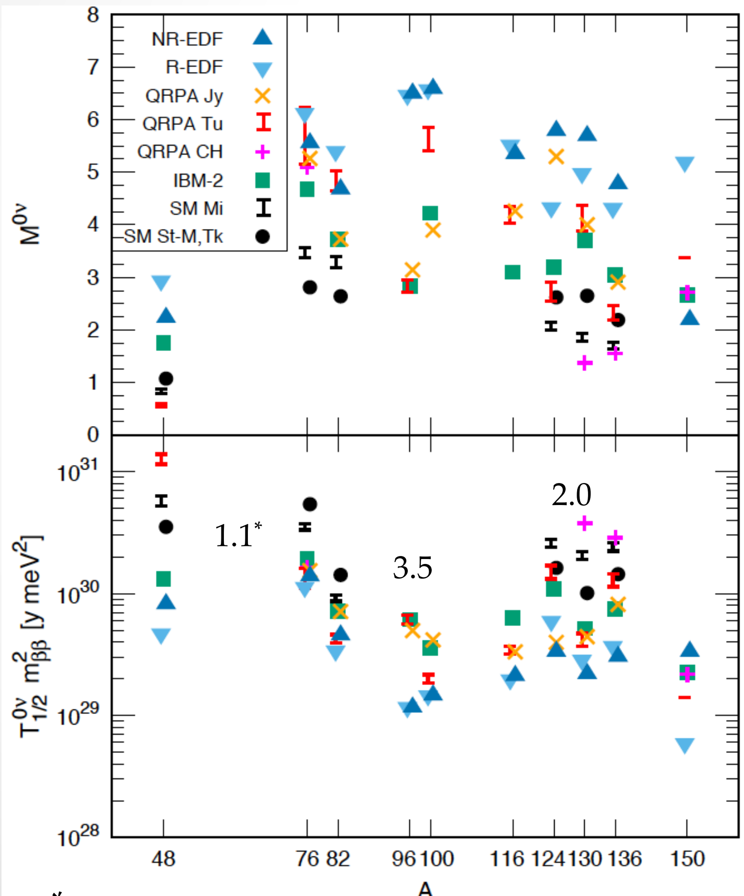

✓**Calculations (still sizeable uncertainties)**: QRPA, Large scale shell model, IBM-2 …..

✓**Measurements** (still not conclusive for 0νββ):

- (π^+, π^-)
- single charge exchange (^{3}He,t)
- electron capture
- transfer reactions …

No isotope significantly preferred when comparing decay rate per mass

Choice mainly driven by experimental considerations

*number = signal rate per 1000 kg yr exposure & for middle of NME values for For $\langle m_{ee}\rangle$ = 17.5 meV ('bottom of IH' for g_A=1.25, $\sin^2\theta_{12}$ = 0.318)

Engel & Menédez

arXiv:1610.06548v2

Courtesy of Stefan Schönert

Experiments

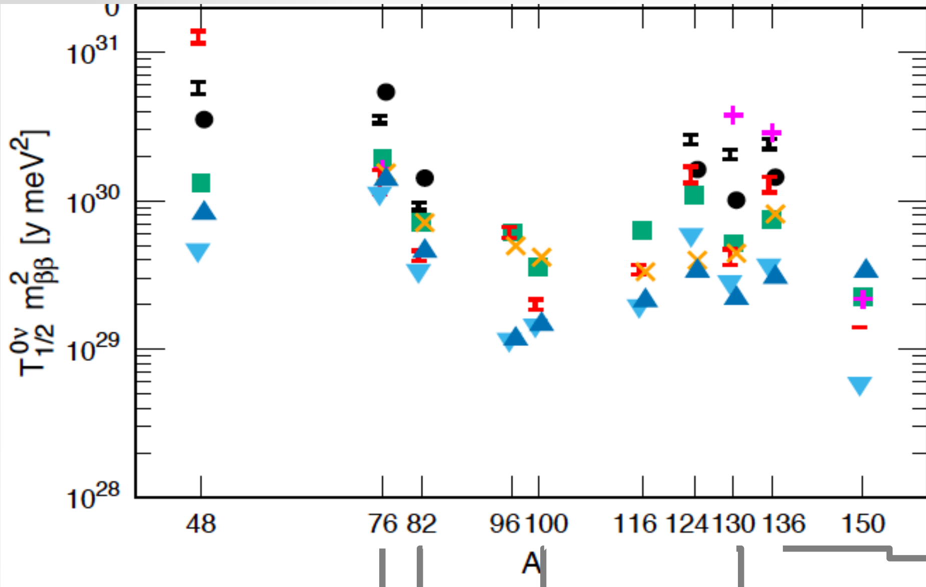

LXe TPC:	EXO-200 / nEXO
gas-Xe TPC:	NEXT, PandaX-III
Xe-loaded LS:	KamLAND-Zen

Te-loaded LS:	SNO+
Te-bolometers:	CUORE / CUPID-Te

Mo-bolometers:	CUPID-Mo (ex Lumineu)
	AMoRE

Se-bolometers:	CUPID-0 (CUPID-Se)
Se-calo-tracko:	SuperNEMO

Ge-semiconductor: GERDA, MJD, LEGEND

& other interesting, but less advanced R&D; ^{48}Ca, ^{150}Nd not available in large quantities

Courtesy of Stefan Schönert

The Idea:

HI-DCE as experimental tool

NUMEN

NUclear **M**atrix **E**lement towards
Neutrinoless *ββ* decay

The challenge: to access quantitative informations

Heavy Ion Double Charge Exchange

1. Induced by strong interaction

2. Sequential nucleon transfer mechanism 4^{th} order:
   Brink's Kinematical matching conditions
   D.M.Brink, et al., Phys. Lett. B 40 (1972) 37

3. Meson exchange mechanism 2^{nd} order

4. Possibility to go in both directions

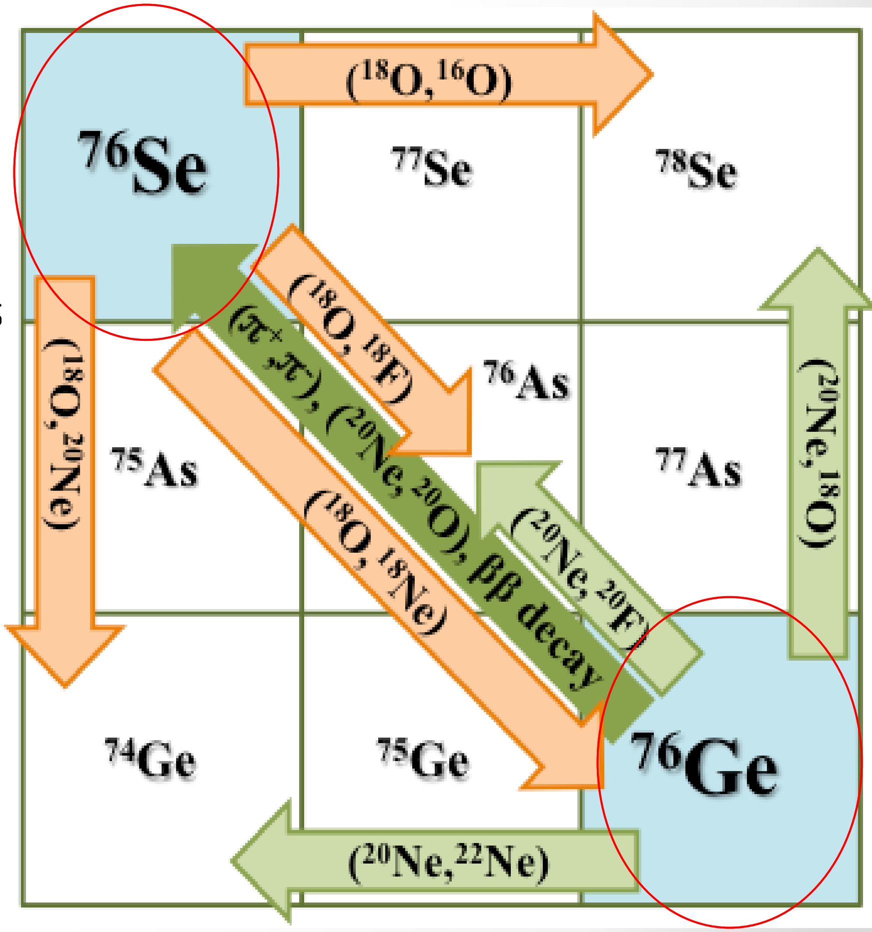

HI–DCE reactions vs $0\nu\beta\beta$ decay

Differences

- DCE mediated by **strong interaction**, $0\nu\beta\beta$ by **weak interaction**
- DCE includes **sequential** multinucleon transfer **mechanism**

Similarities

- **Same initial and final states:** Parent/daughter states of the $0\nu\beta\beta$ decay are the same as those of the target/residual nuclei in the DCE
- **Similar operator:** Fermi, Gamow-Teller and rank-2 tensor components are present in both the transition operators, with tunable weight in DCE
- **Large linear momentum** (~100 MeV/c) available in the virtual intermediate channel
- **Non-local** processes: characterized by two vertices localized in a pair of valence nucleons
- **Same nuclear medium**: Constraint on the theoretical determination of quenching phenomena on $0\nu\beta\beta$
- **Off-shell propagation** through virtual intermediate channels

A good linear correlation between double GT transitions to the ground state of the final nucleus and $0\nu\beta\beta$ decay NMEs is reported for pf-shell nuclei in ref.:
J. *Menéndez, N. Shimizu and K. Yako, arXiv:1712.08691v1.* ; *N. Shimizu, J. Menéndez and K. Yako, arXiv:1709:01088.*

Few experimental attempts

First pioneering explorations of HI – DCE in the 80s at energies above the Coulomb barrier in: Berkeley, NSCL-MSU, IPN-Orsay, Los Alamos to determine the mass of n-rich isotopes by reaction Q-value measurements

- **not conclusive because** of the very poor yields in the measured energy spectra and the lack of angular distributions, due to the **very low cross-sections** involved.
- not easy to measure, in the same experimental conditions, the **different competitive reaction channels** (limit due to the prohibitive small cross-sections).

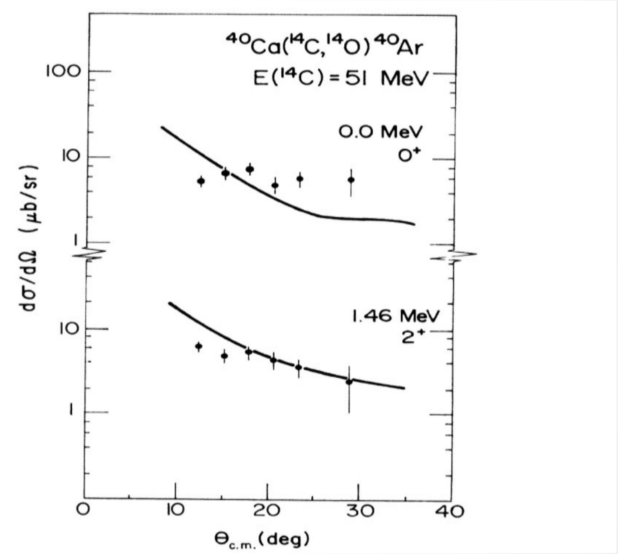

$^{40}Ca(^{14}C,^{14}O)^{40}Ar$ @ 51 MeV

Recently at RIKEN and RCNP (80-200 MeV/u):

- (^{8}He,^{8}Be) was used to search for the tetra-neutron (4n) system, *K. Kisamori et al., Phys. Rev. Lett. 116, 052501 (2016).*
- (^{11}B,^{11}Li) and (^{12}C,^{12}Be) were used to find the DGT resonance, *H. Sagawa, T. Uesaka, Phys. Rev. C 94, 064325 (2016).*

The facility: DCE @ LNS

K800 Superconducting Cyclotron

- In operation since 1996.
- Accelerates from H to U ions
- Maximum energy 80 MeV/u.

MAGNEX spectrometer

F. Cappuzzello et al., Eur. Phys. J. A (2016) 52: 167

crucial for the experimental challanges !

Optical characteristics	Current values
Maximum magnetic rigidity (Tm)	1.8
Solid angle (msr)	50
Momentum acceptance	-14%, +10%
Momentum dispersion (cm/%)	3.68

Good compensation of the aberrations: Trajectory reconstruction

Measured resolutions:
- Energy $\Delta E/E \sim 1/1000$
- Angle $\Delta\theta \sim 0.2°$
- Mass $\Delta m/m \sim 1/160$

DCE @ INFN - LNS

$^{40}Ca(^{18}O,^{18}Ne)^{40}Ar$ @ 270 MeV

$0° < \theta_{lab} < 10°$ $Q = -5.9$ MeV

- ^{18}O and ^{18}Ne belong to the same multiplet in S and T
- Very low polarizability of core ^{16}O
- Sequential transfer processes very mismatched $Q_{opt} \sim 50$ MeV
- Doubly magic target

DCE @ LNS

$^{40}Ca(^{18}O,^{18}Ne)^{40}Ar$ @ 270 MeV $0° < \theta_{lab} < 10°$ $Q = -5.9$ MeV

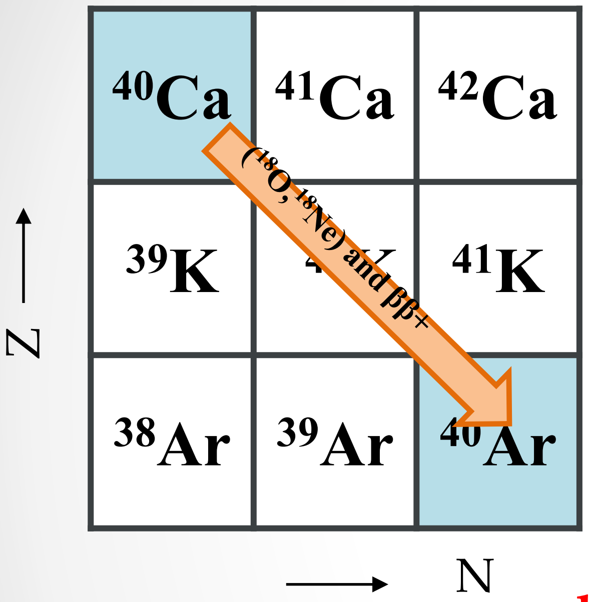

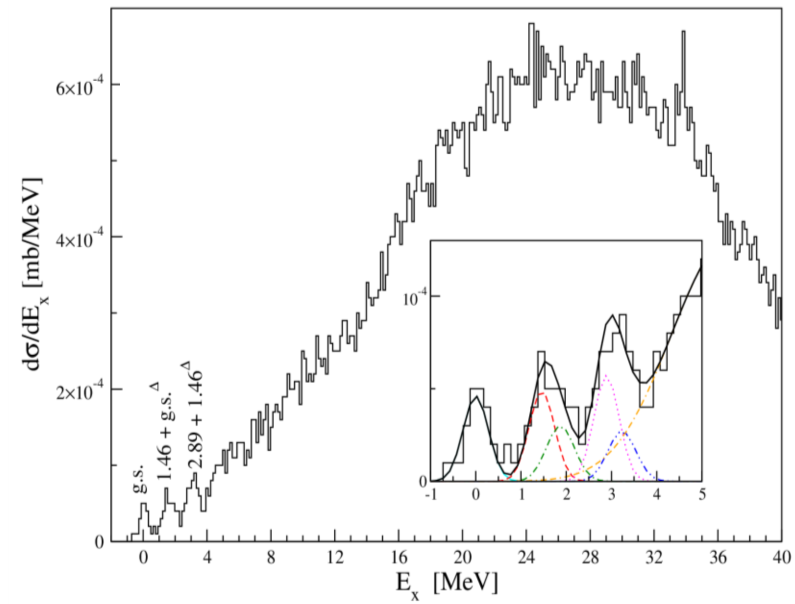

$d\sigma^{DCE}/d\Omega = 11\mu b/sr$ at $\theta_{cm} = 0^0$

- **Experimental feasibility:** zero-deg, resolution (500 keV), low cross-section (μb/sr)
  Limitations of the past HI-DCE experiments are overcome!

- **Data analysis feasibility**: the analysis of the DCE cross-section has lead to NME compatible with the existing calculations

F. Cappuzzello, et al. Eur. Phys. J. A (2015) 51: 145

$$\left|M^{DCE}_{\sigma\tau}\left(^{40}Ca\right)\right|^2 = 0.24 \pm 0.12$$

$$\left|M^{DCE}_{\tau}\left(^{40}Ca\right)\right|^2 = 0.22 \pm 0.11$$

The role of the competing processes

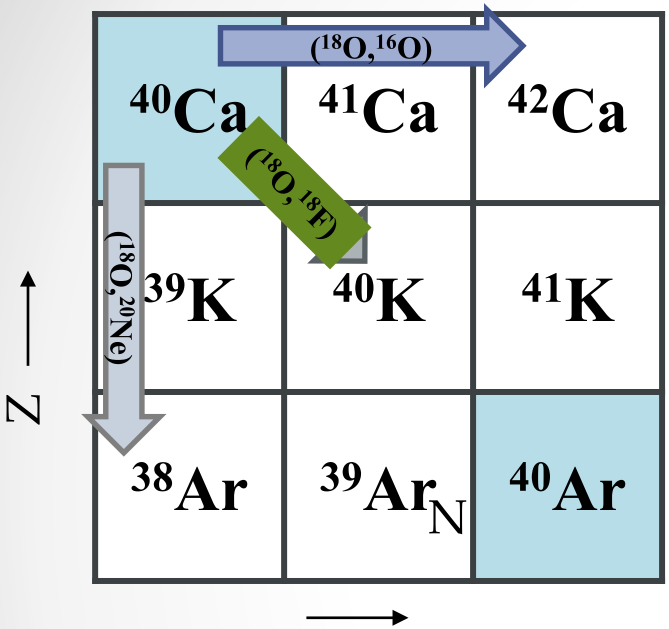

F. Cappuzzello et al. Eur. Phys. J. A (2015) 51: 145

2p-transfer

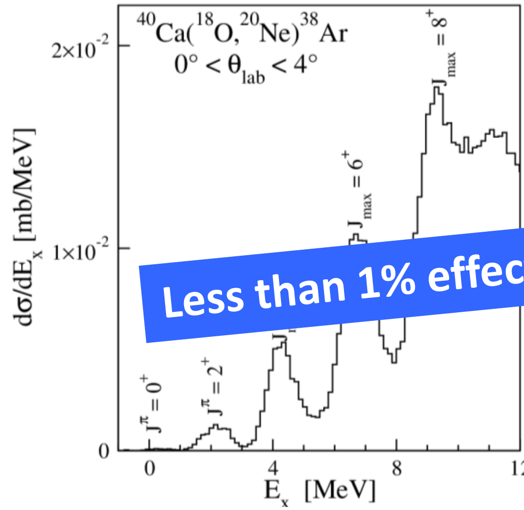

2n-transfer

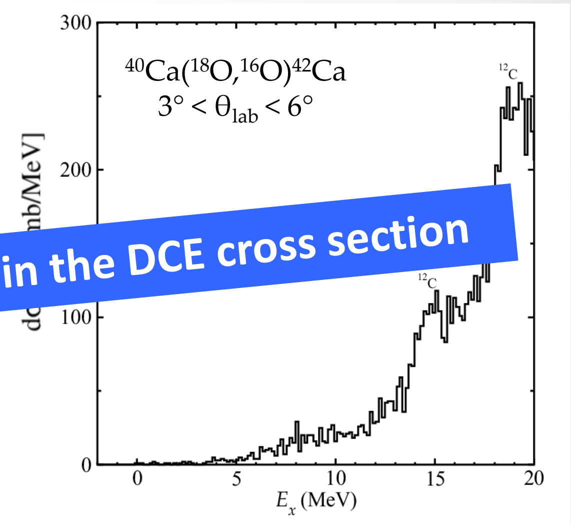

Less than 1% effect in the DCE cross section

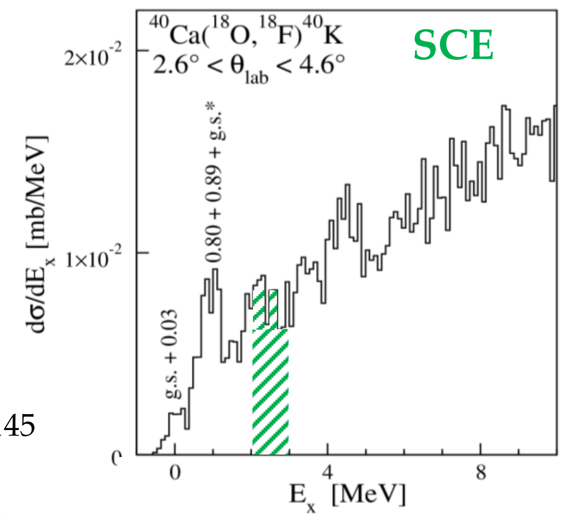

x-section ($2MeV < E_x < 3MeV$)
≈ 0.5 mb/sr

Extracted B(GT) = 0.087 ± 0.02
B(GT) from (^3He,t) = 0.083
Y. Fujita

Moving towards hot-cases

(^{76}Ge, ^{116}Cd, ^{130}Te, ^{136}Xe, …)

- Reaction Q-values normally more negative than in the ^{40}Ca case
- (^{18}O,^{18}Ne) reaction particularly advantageous, but is of *$\beta^+\beta^+$ kind*

  Reactions of *$\beta^-\beta^-$ kind* are not as favourable as the (^{18}O,^{18}Ne):
  - (^{18}Ne,^{18}O) requires a radioactive beam
  - (^{20}Ne,^{20}O) or (^{12}C,^{12}Be) have smaller B(GT)
- In some cases gas or implanted target necessary (e.g. ^{136}Xe or ^{130}Xe)
- In some cases MAGNEX energy resolution is not enough to separate the g.s. from the excited states in the final nucleus → Detection of γ-rays

Much higher beam current is needed !

NUMEN experiment programs

(^{18}O , ^{18}Ne) → $\beta^+\beta^+$

(^{20}Ne, ^{20}O) → $\beta^-\beta^-$

- Beams intensity up to 10^{14} pps
- Energy range 15-70 MeV/u
- Beam power range 1-10 kW

The phases of the NUMEN project

a long range time perspective

- ***Phase1: the experiment feasibility***

  - $^{40}Ca(^{18}O,^{18}Ne)^{40}Ar$ @ 270 MeV already done: the results demostrate the technique feasibility.

- ***Phase2: toward "hot" cases optimizing experimental conditions and getting first result***

  - Few experiments on selected isotopes candidate for $0\nu\beta\beta$ decay (integrated harge of tens of mC)
  - R&D on CS and MAGNEX, preserving the access to the present facility
  - Theoretical model developments.

- ***Phase3: the facility upgrade***

  - Disassembling of the old set-up and re-assembling of the new ones will start (18-24 months)
  - Tests of new detectors (Tandem @ LNS and other Laboratories)

- ***Phase4: the systematic experimental campaign***

  - Systematic experimental campaign with high beam intensities (some pμA; integrated charge of hundreds of mC up to C) on all the isotopes candidates for $0\nu\beta\beta$ decay

Tentative time table

year	2013	2014	2015	2016	2017	2018	2019	2020	2021
Phase1	done								
Phase2				Approved					
Phase3									
Phase4									

The NUMEN goals

1. **Holy Graal**: sudying if **the σ^{DCE}** and in **turn NME_{DCE} are connected to** ***$0\nu\beta\beta$*** **NMEs as a smooth function of E_p and A** → require the development of the reaction and nuclear structure theory and a systematic set of data.

2. A new generation of **DCE constrained to $0\nu\beta\beta$ NME theoretical calculations** achievable in a short term with a reduced dataset

3. To provide **relative NME information on the different candidate isotopes** for the *$0\nu\beta\beta$* decay : the ratio of the σ^{DCE} can give **a model independent way** to compare the sensitivity of different half-life experiment

GERDA ^{76}Ge

CUORE ^{130}Te

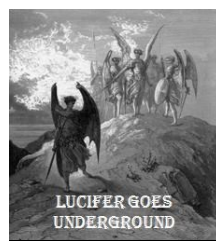

^{82}Se

Enriched Xenon Observatory EXO for double beta decay ^{136}Xe

^{116}Cd

strong impact in future development of the field, looking for a "golden isotope" …

NUMEN phase 2

- R&D for upgrade @ LNS facilities

- Detector R&D : new MAGNEX focal plane detector for PID and tracker ;
  new target development
  electronic development ;

- Theoretical model developments.

- Long run @ LNS with MAGNEX with few isotopes, candidates for $0\nu\beta\beta$ already at our reach in terms of energy resolution and availability of thin targets

European Commission — Horizon 2020 European Union funding for Research & Innovation — erc

ERC Starting Grant 2016

enhance the project discovery potential already in NUMEN phase 2

NUMEN phase 2 R&D: upgrade @ LNS facilities

- **Upgrade of the LNS accelerator and beam lines**

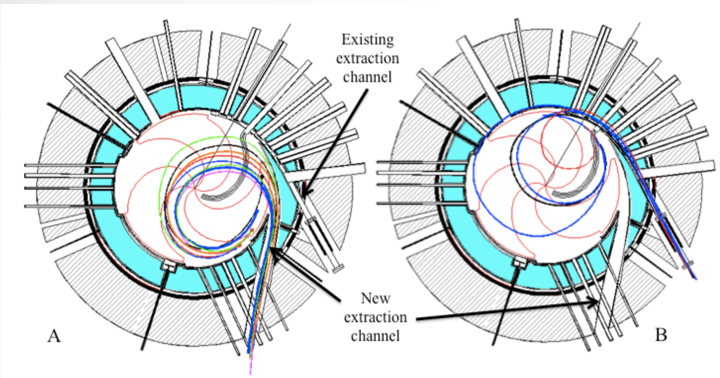

- **CS** accelerator current (from 100 W to 5-10 kW); from elecrostatic to extraction by stripping
- **beam transport line** transmission efficiency to nearly 100%. The new beam transport line corresponds with the FRAgment Ion Separation line.

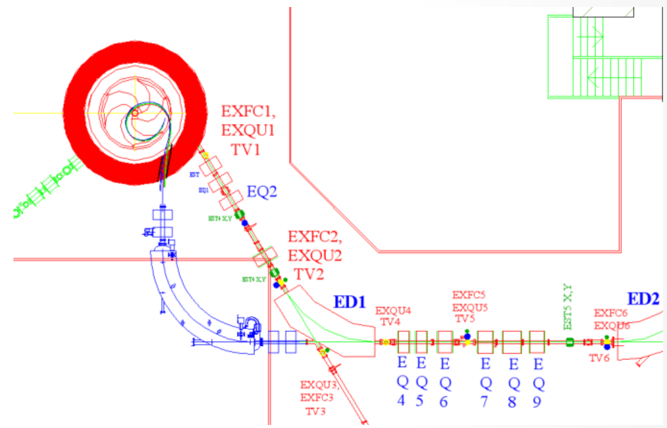

- **Beam dump for the MAGNEX hall**

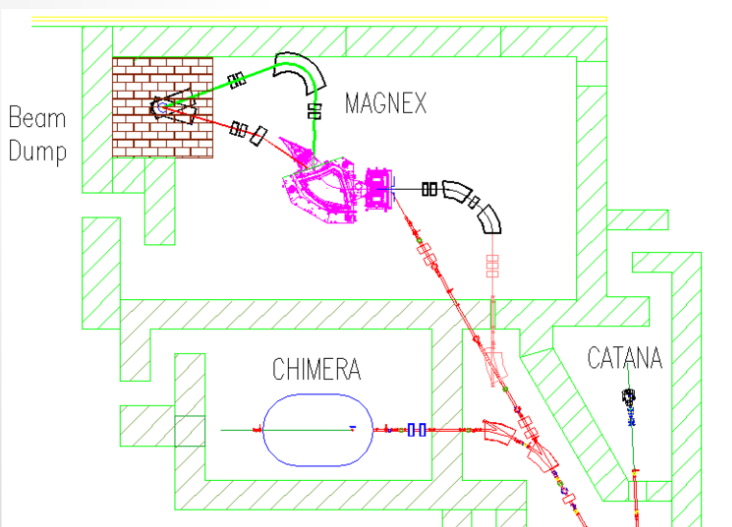

- installed 2.5 meters **below the floor** after a vertical beam line
- 5 x 5 x 5 m^3

NUMEN phase 2 R&D:

MAGNEX major upgrades

➢ **The Focal Plane Detector** (from 2 kHz to several MHz): **hybrid detector**

FROM → **TO**

Gas section: proportional wires and drift chambers
+
Stopping wall of silicon detectors

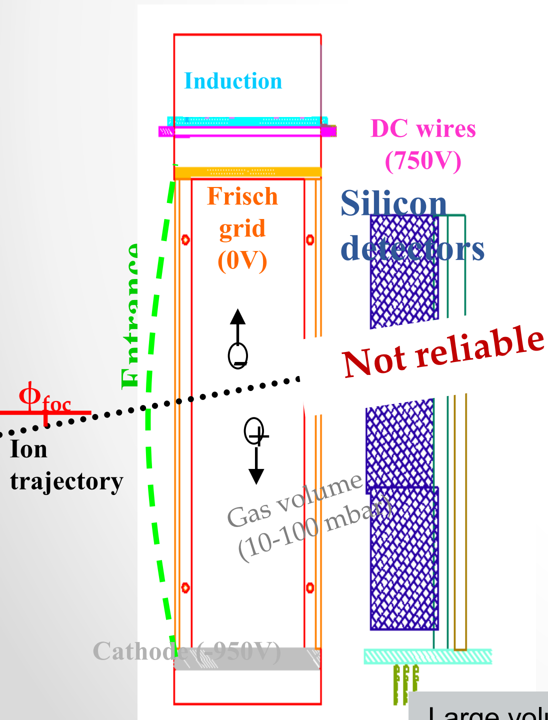

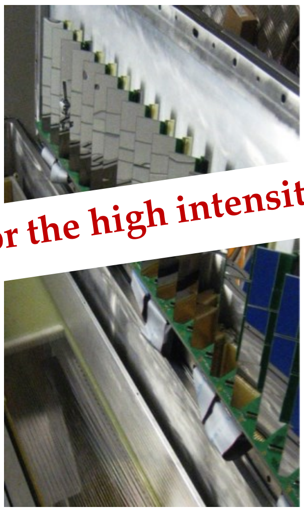

Large volume: 1360mm X 200mm X 96mm

Micro-pattern tracker
+
PID wall

- Radiation hard
- Heavy ions
- Working in gas environment
- Large area
- High energy resolution (2%)
- Timing resolution (few ns)

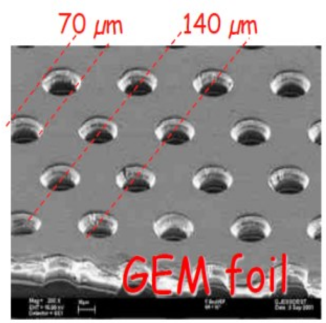

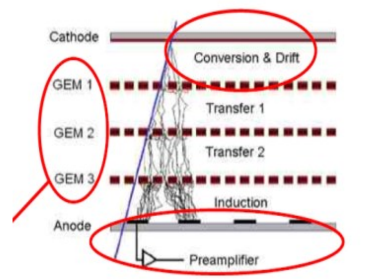

low pressure and **wide dynamic range**

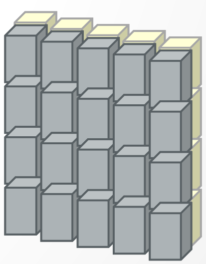

➢ SiC-SiC pad telescopes
➢ Phoswich detectors
➢ SiC (ΔE) + scintillator (E)

NUMEN phase 2 R&D:

MAGNEX major upgrades

➢ **Array of scintillators for γ-rays**

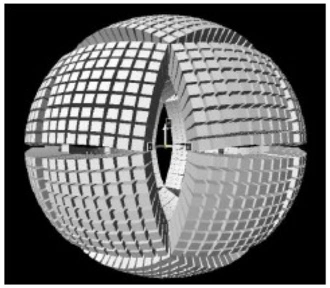

- Measurement in coincidence with MANEX study and simulation still in progress…

➢ **New electronics**

- ASIC front–end chip **VMM2(3)**
- Read – out: new generation of **FPGA** and System On Module (**SOM**)

➢ **Radiation tolerant Targets**

- Evaporation on a **Graphite backing** (good properties)
- **Cooling** system

➢ **Magnets upgrade**

- **Increase** of the maximum **magnetic rigidity** from 1.8 Tm to 2.5 Tm

NUMEN phase 2 experimental activity

Few isotope targets:
energy resolution and availability of thin targets at our rach among isotopes candidates for *0νββ*

Isotope Target for $\beta^-\beta^-$	$E^*(2^+)$ [keV]	Isotope Target for $\beta^+\beta^+$, β^+EC, ECEC decay	$E^*(2^+)$ [keV]
^{48}Ca*	3832	^{48}Ti	983
^{76}Ge	563	**^{76}Se**	559
^{78}Se	614	^{78}Kr *	455
^{82}Se*	655	^{82}Kr	776
^{92}Zr	934	^{92}Mo *	1509
^{96}Zr*	1582	^{96}Mo	778
^{96}Mo	778	^{96}Ru *	833
^{100}Mo*	536	^{100}Ru	539
^{106}Pd	512	**^{106}Cd**	633
^{110}Pd*	374	^{110}Cd	658
^{116}Cd	513	**^{116}Sn**	1294
^{124}Sn*	1132	^{124}Te	603
^{124}Te	603	^{124}Xe *	354
^{128}Te*	743	^{128}Xe	443
^{130}Te	840	^{130}Xe	536
^{130}Xe	536	^{130}Ba *	357
^{136}Xe*	1313	^{136}Ba	818
^{136}Ba	818	^{136}Ce *	552
^{148}Nd*	302	^{148}Sm	550
^{150}Nd*	130	^{150}Sm	334
^{154}Sm*	82	^{154}Gd	123
^{160}Gd*	75	^{160}Dy	87
^{198}Pt*	407	^{198}Hg	412

NUMEN runs - Phase 2

^{116}Cd - ^{116}Sn case

- Two experiments @ 15 MeV/A
- ^{18}O + ^{116}Sn
- ^{20}Ne + ^{116}Cd

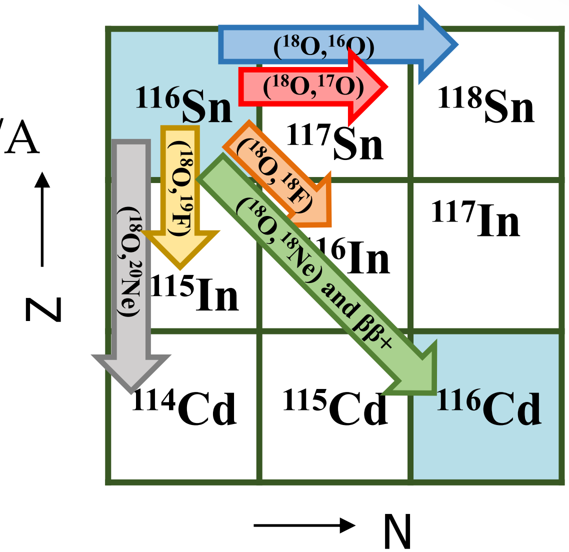

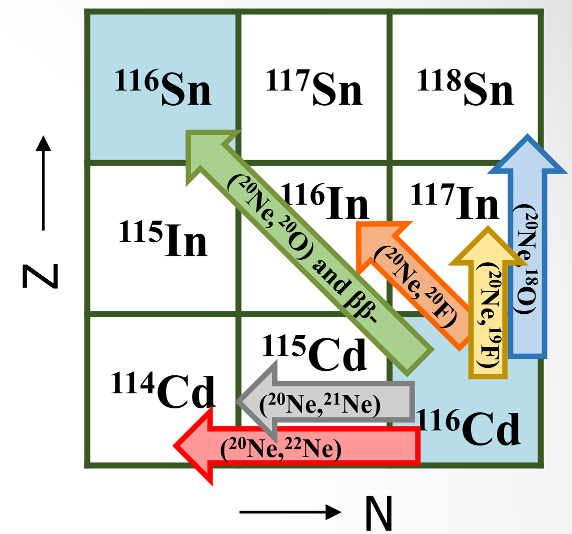

^{130}Te – ^{130}Xe case

- One experiment @ 15 MeV/A
- ^{20}Ne + ^{130}Te

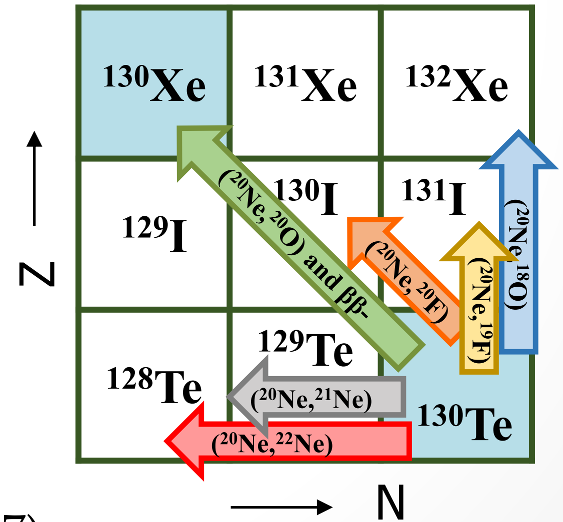

^{76}Ge – ^{76}Se case

- One experiment @ 15 MeV (November 2017)
- ^{20}Ne + ^{76}Ge

The $^{116}Cd(^{20}Ne,^{20}O)^{116}Sn$ reaction

- $^{20}Ne^{10+}$ beam at 15 AMeV incident energy delivered by CS accelerator
- ^{116}Cd rolled target, 1370 μg/cm^2 thickness
- Ejectiles detected by the MAGNEX large acceptance spectrometer
- Angular acceptance $3° < \theta < 14°$

Measured channels

- DCE reaction $^{116}Cd(^{20}Ne,^{20}O)^{116}Sn$
- CEX reaction $^{116}Cd(^{20}Ne,^{20}F)^{116}In$
- 2p-transfer $^{116}Cd(^{20}Ne,^{18}O)^{118}Sn$
- 2n-transfer $^{116}Cd(^{20}Ne,^{22}Ne)^{114}Cd$
- 1p-transfer $^{116}Cd(^{20}Ne,^{19}F)^{117}In$
- 1n-transfer $^{116}Cd(^{20}Ne,^{21}Ne)^{115}Cd$

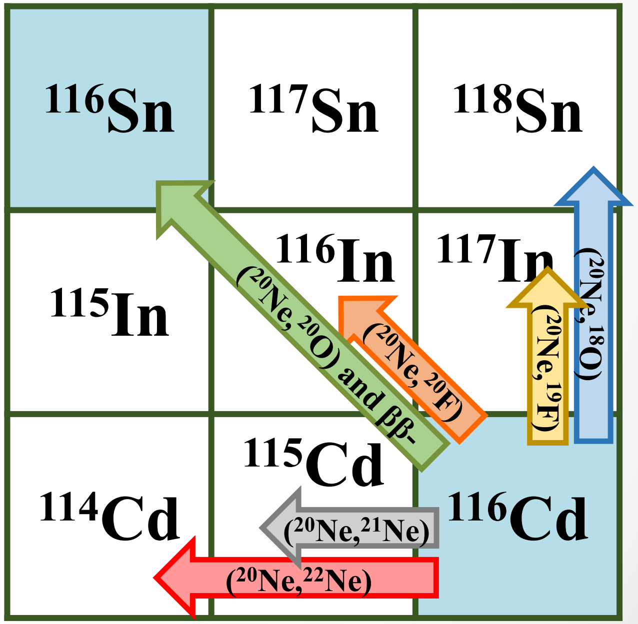

Experimental results

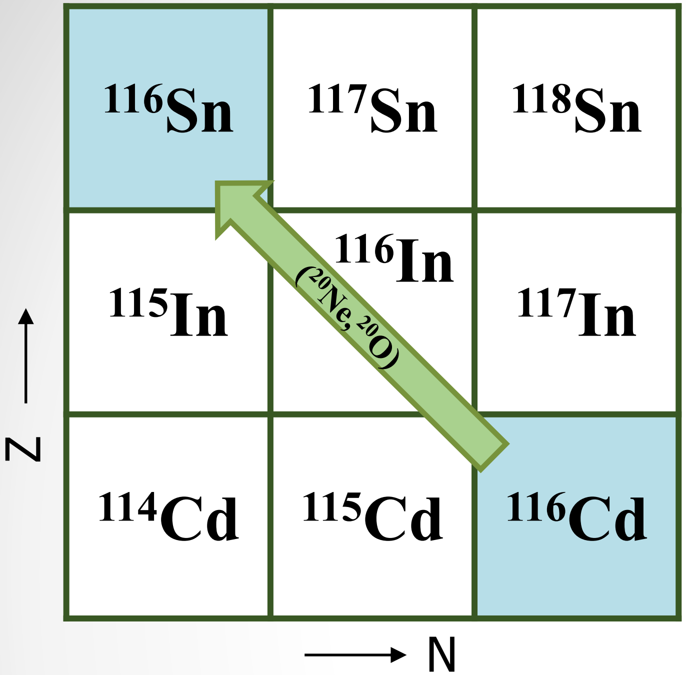

DCE reaction $^{116}Cd(^{20}Ne,^{20}O)^{116}Sn$

- Absolute cross section measured
- g.s. → g.s. transition isolated

* ^{20}O excitation at 1.673 MeV (2^+)

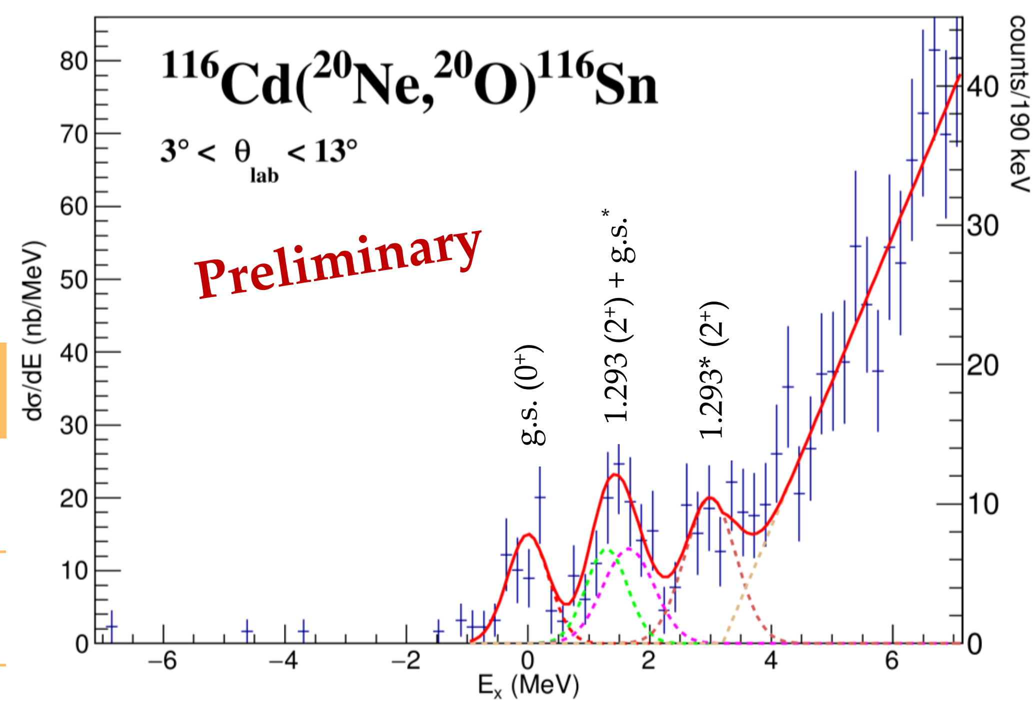

State (MeV)	Counts	Absolute cross section (nb)
$^{116}Sn_{gs}\ (0^+) + {}^{20}O_{gs}\ (0^+)$	31	12 ± 2
$^{116}Sn_{1.293}\ (2^+) + {}^{20}O_{gs}\ (0^+)$ $^{116}Sn_{gs}\ (0^+) + {}^{20}O_{1.673}\ (2^+)$	63	25 ± 3
$^{116}Sn_{1.293}\ (2^+) + {}^{20}O_{1.673}\ (2^+)$		21 ± 2

Resolution ~ 800 keV FWHM

Experimental results

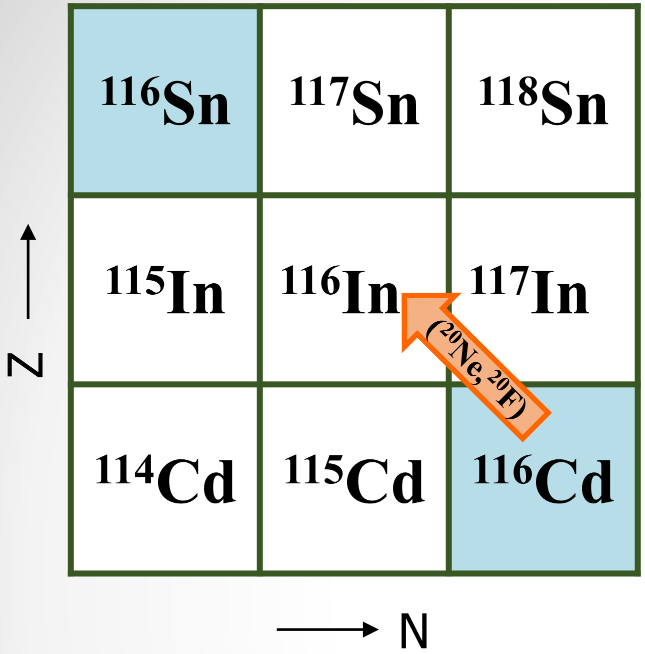

SCE reaction $^{116}Cd(^{20}Ne,^{20}F)^{116}In$

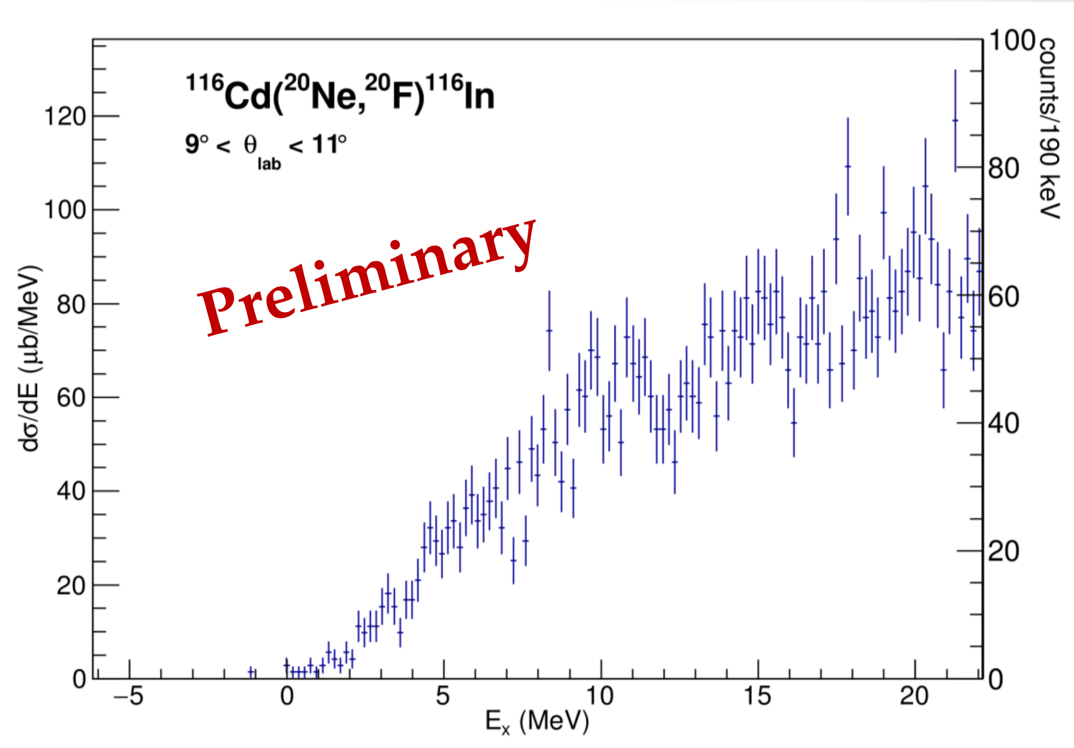

^{116}In

E_x (MeV)	J^π
g.s.	1^+
0.127	5^+
0.223	4^+
0.272	2^+
0.289	8^-

^{20}F

E_x (MeV)	J^π
g.s.	2^+
0.656	3^+
0.822	4^+
0.983	1^-

High level density in residual and ejectile

- **Population of high multipolarity states**
- **Multipole decomposition analysis needed**

Experimental results

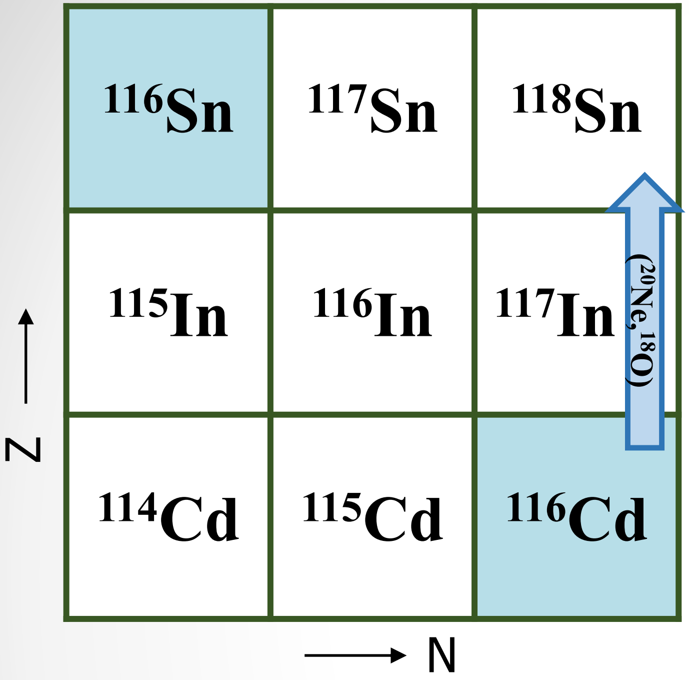

2p-transfer $^{116}Cd(^{20}Ne,^{18}O)^{118}Sn$

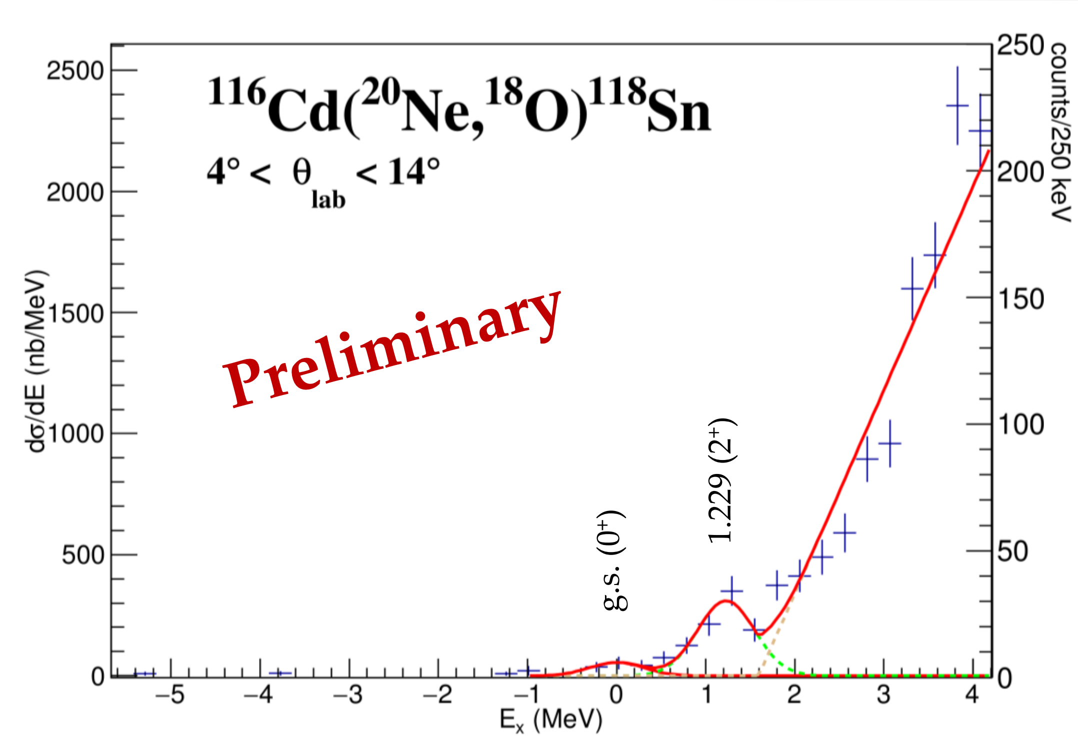

State (MeV)	Counts	Absolute cross section (nb)
g.s. (0^+)	11	33 ± 10

A **peak** corresponding to **g.s. transition** is visible despite the very low statistic. The FWHM resolution is ~800 keV.

Calculation for multi-nucleon transfer

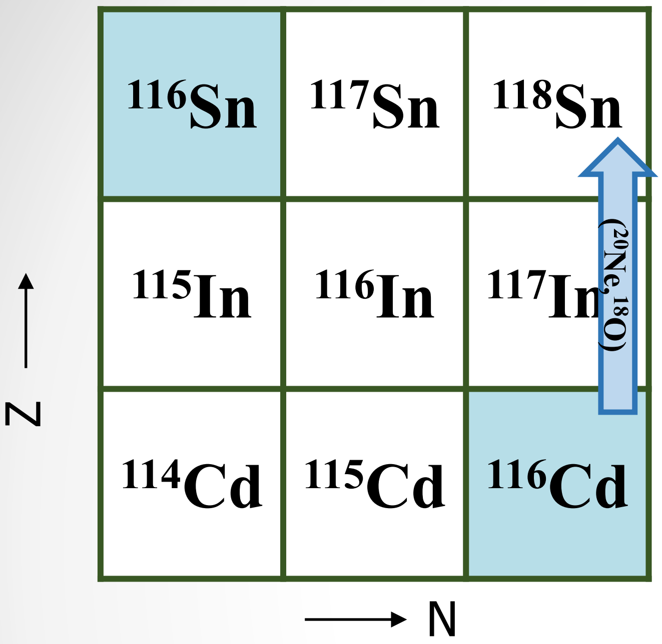

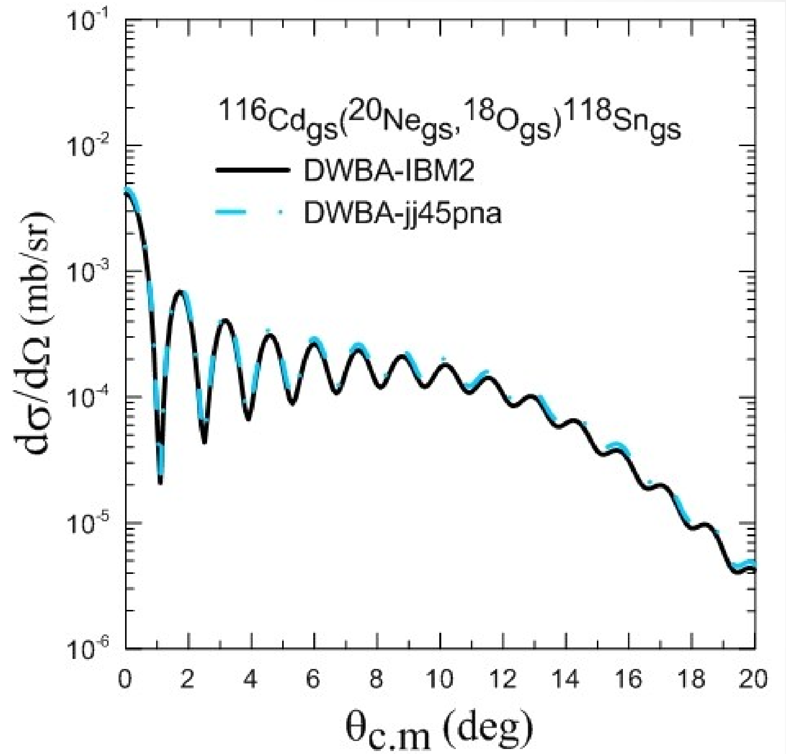

State (MeV)	Measured cross section (nb)	Calculated cross section (nb)
g.s. (0^+)	33± 10	26

Calculation for multi-nucleon transfer

The role of multi-nucleon transfer routes

vs

The diagonal process (experimental cross section 12 ± 2 nb)

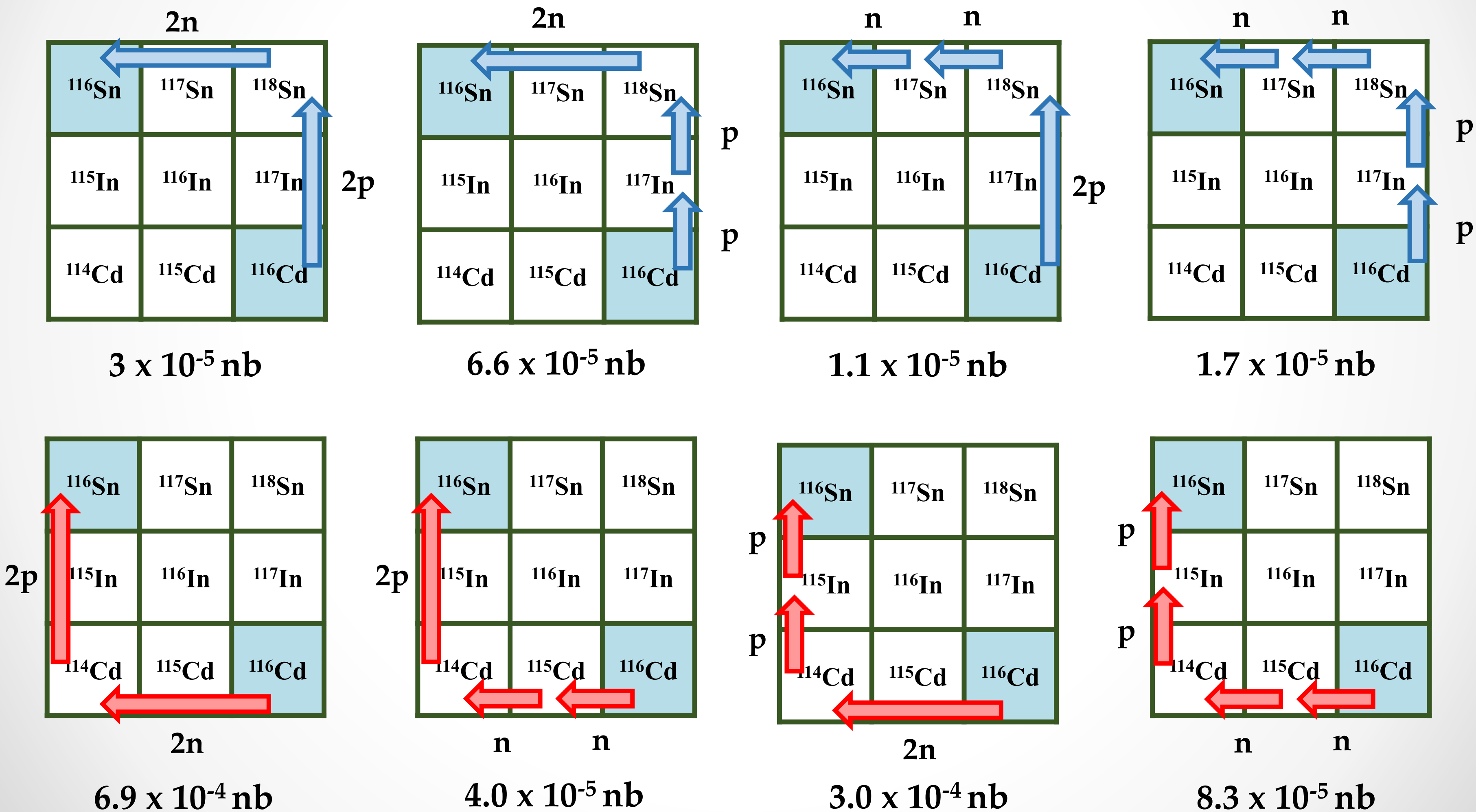

Calculation for multi-nucleon transfer

The role of multi-nucleon transfer routes

vs

The diagonal process (experimental cross section 12 ± 2 nb)

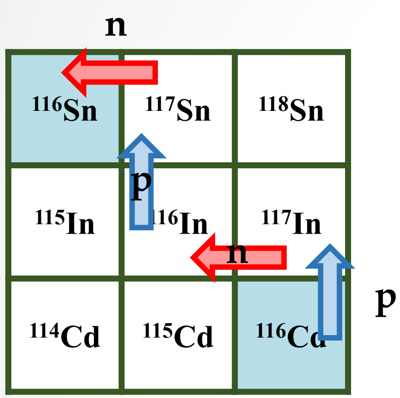

9.4×10^{-8} nb

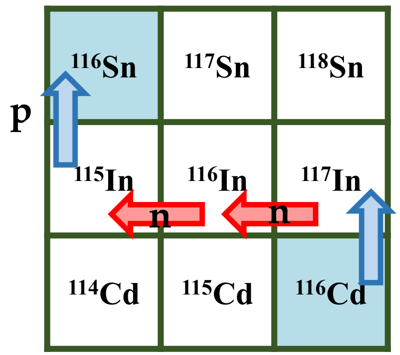

1.5×10^{-6} nb

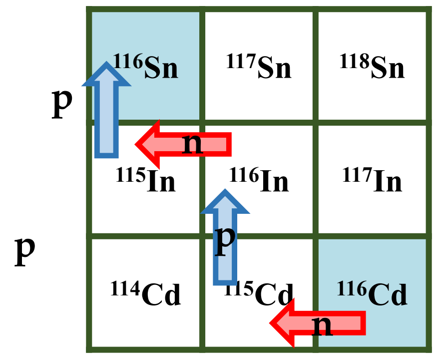

3.2×10^{-7} nb

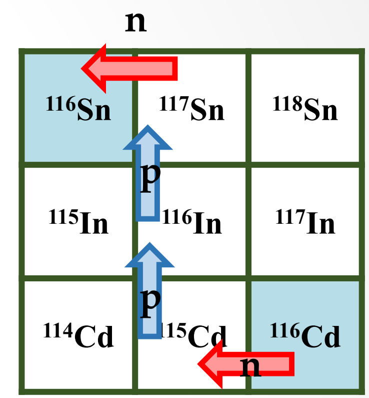

1.1×10^{-7} nb

We can rule out the contribution of multi-nucleon transfer on the diagonal DCE process

The NUMEN collaboration

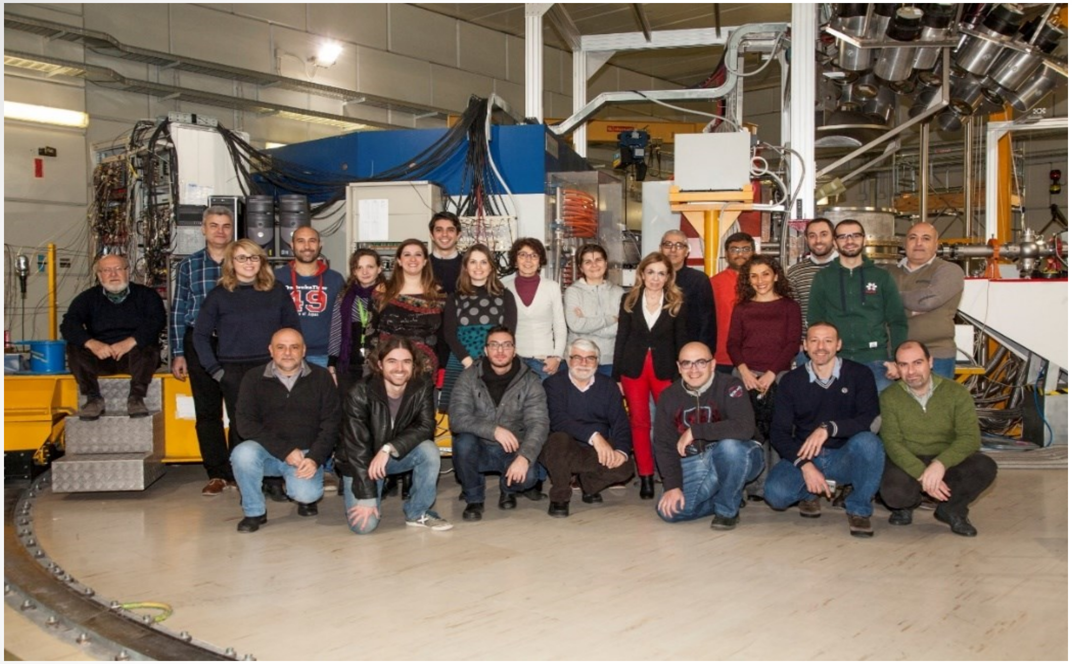

L. Acosta, *C. Agodi*, N. Auerbach, J. Bellone, R. Bijker, D. Bonanno, D. Bongiovanni, T. Borello-Lewin, I. Boztosun, V. Branchina, S. Burrello, M.P. Bussa, S. Calabrese, L. Calabretta, A. Calanna, D. Calvo, *F. Cappuzzello*, D. Carbone, M. Cavallaro, E.R. Chávez Lomelí, A. Coban, M. Colonna, G. D'Agostino, G. De Geronimo, F. Delaunay, N. Deshmukh, P.N. de Faria, C. Ferraresi, J.L. Ferreira, P. Finocchiaro, M. Fisichella, A. Foti, G. Gallo, H. Garcia, G. Giraudo, V. Greco, A. Hacisalihoglu, J. Kotila, F. Iazzi, R. Introzzi, G. Lanzalone, A. Lavagno, F. La Via, J.A. Lay, H. Lenske, R. Linares, G. Litrico, F. Longhitano, D. Lo Presti, J. Lubian, N. Medina, D. R. Mendes, A. Muoio, J. R. B. Oliveira, A. Pakou, L. Pandola, H. Petrascu, F. Pinna, S. Reito, D. Rifuggiato, M.R.D. Rodrigues, A. D. Russo, G. Russo, G. Santagati, E. Santopinto, A. Spatafora, O. Sgouros, S.O. Solakcı, G. Souliotis, V. Soukeras, D. Torresi, S. Tudisco, R.I.M. Vsevolodovna, R. Wheadon, A. Yildirin, V. A. B. Zagatto

77 Researchers
19 Institutions
12 countries

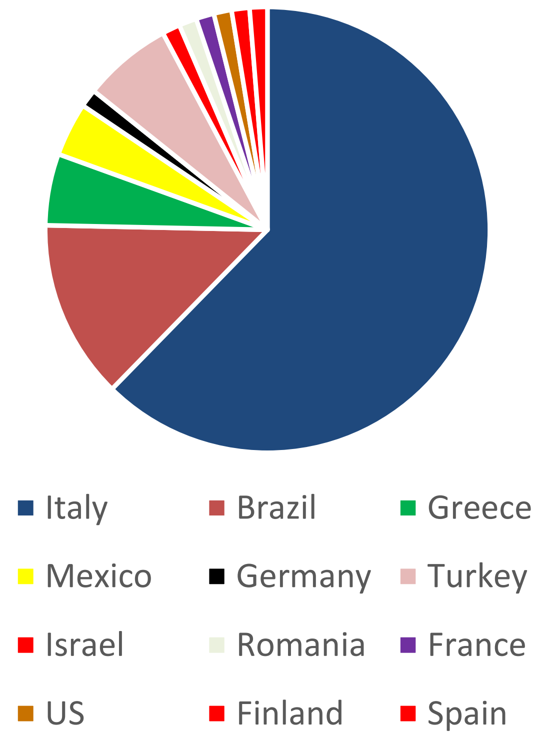

Conclusions and Outlook

- The NUMEN project propose as a tool HI-DCE cross sections towards determination of NME for *$0\nu\beta\beta$*

- First experiments of NUMEN phase2 @ LNS :

- **Good energy resolution to isolate the g.s. → g.s. transition**
- **Absolute cross section measured**
- **Role of multi-nucleon transfer routes negligible with respect to the diagonal DCE**

" The NUMEN project " a paper has been submitted to EPJA

High beam intensity is the new frontier for these challenging studies !


Thank you!

SPARE

Factorization of the charge exchange cross-section

for single CEX:

$$B(\alpha) = \frac{1}{2J_i + 1} |M(\alpha)|^2$$

β-decay transition strengths (reduced matrix elements)

α= Fermi (F)
or Gamow Teller (GT)

$$\frac{d\sigma}{d\Omega}(q,\omega) = \hat{\sigma}_\alpha(E_p, A) F_\alpha(q,\omega) B_T(\alpha) B_P(\alpha)$$

C.J Guess,et al, PRC 83 064318 (2011)

unit cross-section

$$\hat{\sigma}(E_p, A) = K(E_p, 0)|J_\alpha|^2 N_\alpha^D$$

T.N.Taddeucci, et al, Nucl. Phys. A 469 (1987) 125

The factor $F_\alpha(q,\omega)$ describes the shape of the cross-section distribution as a function of the linear momentum transfer and the excitation energy.

(d,^{2}He)

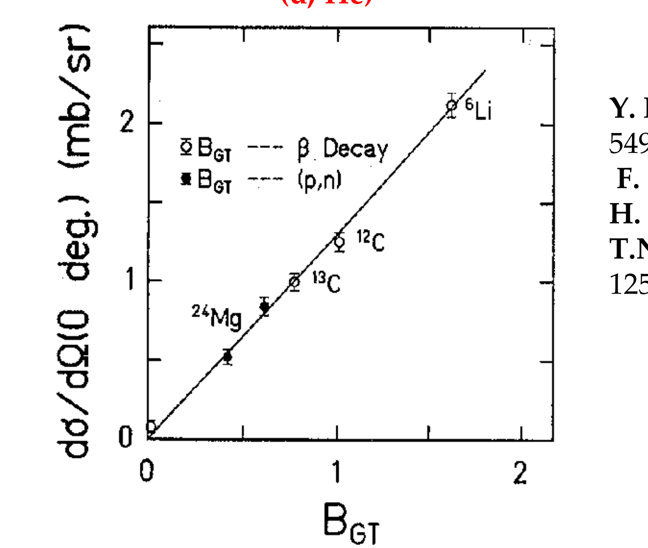

Fig. 12. The measured cm cross-sections of the (d,^{2}He) reactions at 0° as a function of the GT strengths deduced from β-decay or (p,n) reaction studies. The solid line is a linear fit to the data [244].

Y. Fujita Prog. Part. Nuc. Phys. 66 (2011) 549
F. Osterfeld Rev. Mod. Phys. 64 (1992) 491
H. Ejiri Phys. Rep. 338 (2000) 256
T.N. Taddeucci Nucl. Phys. A 469 (1997) 125

(^{7}Li,^{7}Be) S. Nakayama PRC 60 (1999) 047303

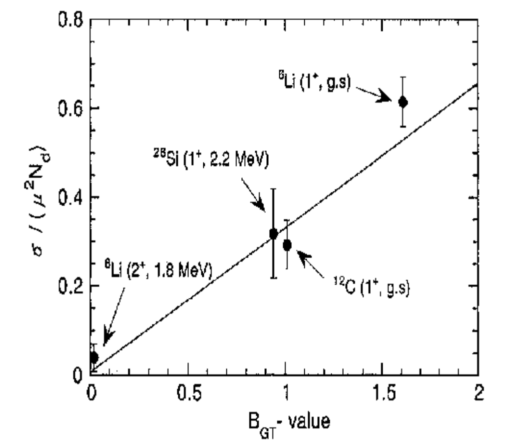

Fig. 18. Cross-sections σ/(μN²) for GT transitions in the (^{7}Li,^{7}Be) reactions at 0° and B(GT) values. μ and N are the reduced mass and the distortion factor, respectively [197].

B(GT;CEX)/B(GT;β-decay) ~ 1 within a few % especially for the strongest transitions

Factorization of the DCE cross section

Under the hypotesis of surface localization, one can assume that the DCE process is just a second order charge exchange: **DCE cross sections can be factorized** in a **nuclear structure term, containing the matrix element,** and a **nuclear reaction factor**.

generalization to DCE:

In analogy to the single charge-exchange, the dependence of the cross-section from q is represented by a Bessel function.

$$\frac{d\sigma^{DCE}}{d\Omega}(q,\omega) = \hat{\sigma}_{\alpha}^{DCE}(E_p, A) F_{\alpha}^{DCE}(q,\omega) B_{T}^{DCE}(\alpha) B_{P}^{DCE}(\alpha)$$

unit cross-section

$$\hat{\sigma}_{\alpha}^{DCE}(E_p, A) = K(E_p, 0) |J_{\alpha}^{DCE}|^2 N_{\alpha}^{D}$$

A wide range of DCE cross sections has never been accurately measured due to :

- The difficult to perform **zero degrees** measurements.
- The poor yields in the measured energy spectra and angular distributions, due to the **very low cross sections**.
- The difficulty to disentangle **possible contributions of multi-nucleon transfer reactions leading to the same final state.**

Energy resolution

In order to separate the ground state-to-ground state transition from that to the first excited state of the residual nucleus, sufficient energy resolution in the measured excitation energy spectra is required. This resolution mainly depends on three factors:

1) the intrinsic energy resolution of the MAGNEX spectrometer ($\delta E_{MAGNEX}/E \sim 1/1000$)
2) the energy spreading of the cyclotron accelerated beam ($\delta E_{CS}/E \sim 1/1000$)
3) contribution due to the straggling and energy loss of the beam and ejectiles in the target film δE_{TARGET}.

δE_{TARGET} depends, for a given beam, on the target film material and thickness and on its uniformity.

Search of 0νββ decay: a worldwide race

List not complete…

Experiment	Isotope	Lab
GERDA	^{76}Ge	LNGS [Italy]
CUORE	^{130}Te	LNGS [Italy]
Majorana	^{76}Ge	SURF [USA]
KamLAND-Zen	^{136}Xe	Kamioka [Japan]
EXO/nEXO	^{136}Xe	WIPP [USA]
CUPID - Lucifer	^{82}Se, ^{100}Mo	LNGS [Italy]
SNO+	^{130}Te	Sudbury [Canada]
SuperNEMO	^{82}Se (or others)	LSM [France]
CANDLES	^{48}Ca	Kamioka [Japan]
COBRA	^{116}Cd	LNGS [Italy]
DCBA	many	[Japan]
AMoRe	^{100}Mo	[Korea]

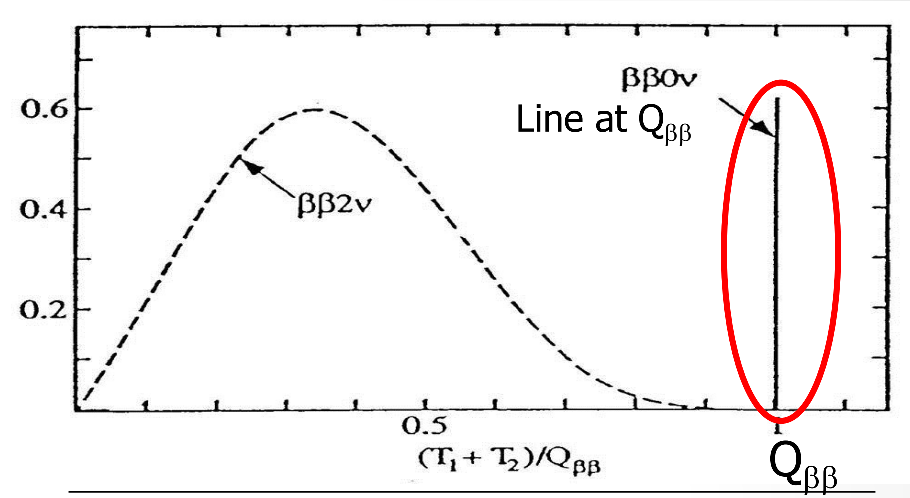

Isotope	$\beta\beta(0\nu)$ Half-life limit (years)	Natural Abundance [%]	Q-value (MeV)
^{48}Ca	$>1.4 \times 10^{22}$ [31]	0.187	4.2737
^{76}Ge	$>3.0 \times 10^{25}$ [32]	7.8	2.0391
^{82}Se	$>1.0 \times 10^{23}$ [33]	9.2	2.9551
^{100}Mo	$>1.1 \times 10^{24}$ [34]	9.6	3.0350
^{130}Te	$>4.0 \times 10^{24}$ [35]	34.5	2.5303
^{136}Xe	$>1.1 \times 10^{25}$ [36]	8.9	2.4578
^{150}Nd	$>1.8 \times 10^{22}$ [37]	5.6	3.3673

R. Henning / Reviews in Physics 1 (2016) 29–35

Nature 544, 47–52 (06 April 2017)
doi:10.1038/nature21717
" Background-free search for neutrinoless Double-βdecay of ^{76}Ge with GERDA "

Nuclear response to the same degrees of freedom by weak and strong interaction: β decay and Single Charge Exchange

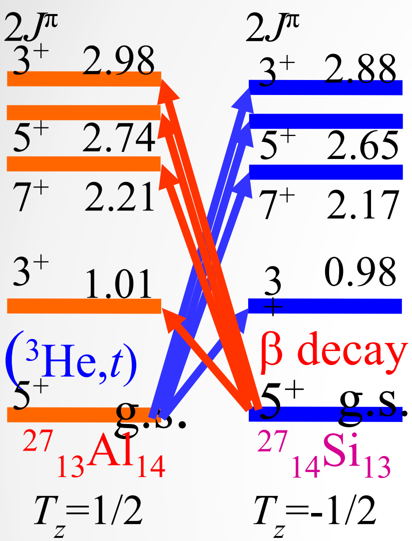

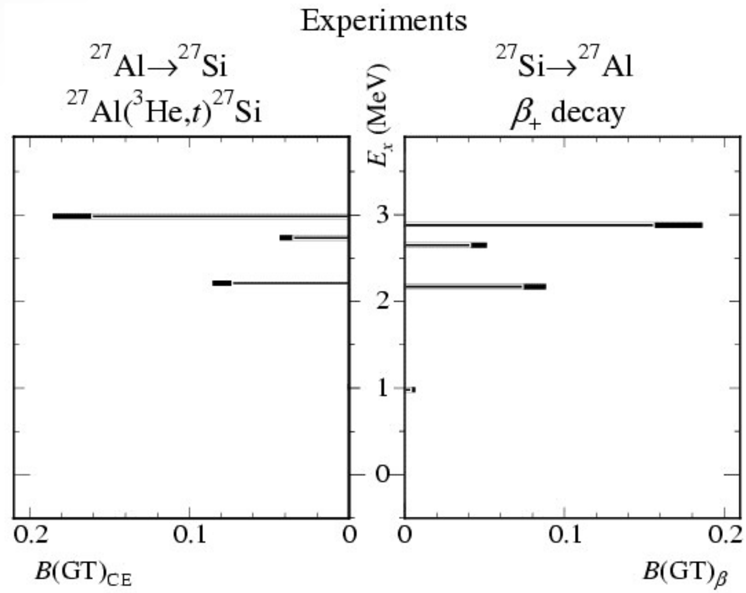

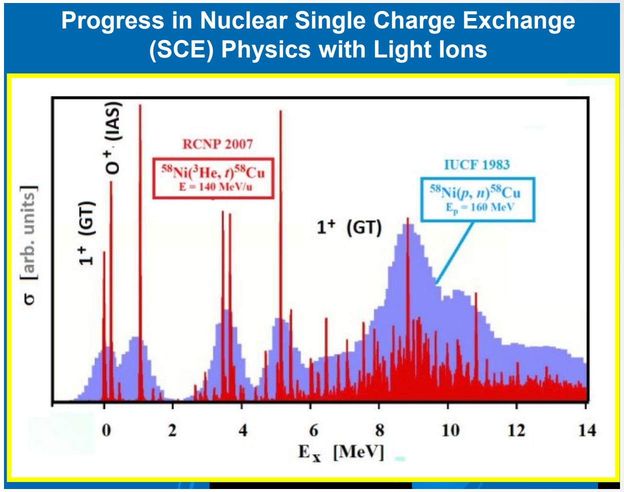

B(GT;CEX)/B(GT;β-decay) ~ 1 within a few %

(d,^{2}He)

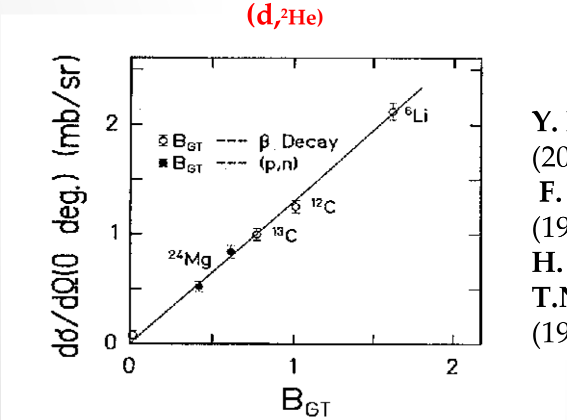

Fig. 12. The measured cm cross-sections of the (d, ^{2}He) reactions at 0° as a function of the G^t strengths deduced from β-decay or (p,n) reaction studies. The solid line is a linear "t to the data [244].

Y. Fujita Prog. Part. Nuc. Phys. 66 (2011) 549
F. Osterfeld Rev. Mod. Phys. 64 (1992) 491
H. Ejiri Phys. Rep. 338 (2000) 256
T.N. Taddeucci Nucl. Phys. A 469 (1997) 125

(^{7}Li,^{7}Be) S. Nakayama PRC 60 (1999) 047303

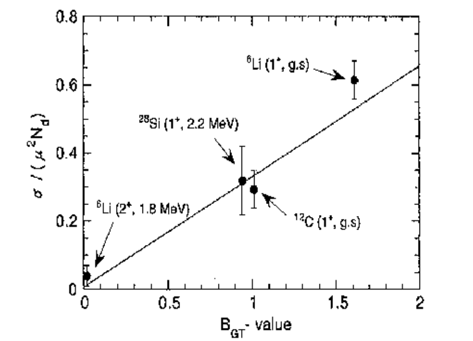

Fig. 18. Cross-sections $\sigma/(\mu N'')$ for G^t transitions in the (^{7}Li,^{7}Be) reactions at 0° and $B(G^t)$ values. μ and N'' are the reduced mass and the distortion factor, respectively [197].

MAGNEX:

large acceptance magnetic spectrometer

Particle Identification

Z Identification

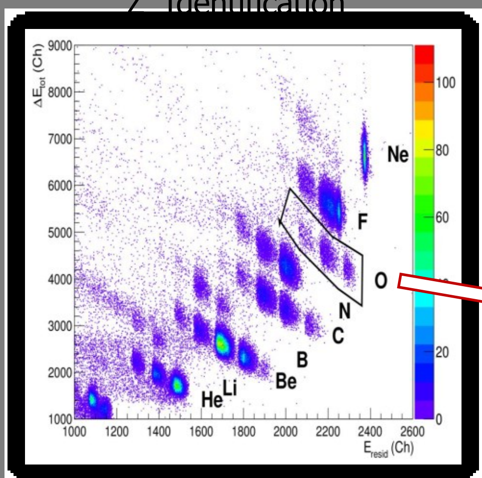

A, q identification

Ion trajectory in a magnetic spectrometer

$$B\rho = \frac{p}{q} \rightarrow X_{foc}^2 \propto \frac{m}{q^2} E_{resid}$$

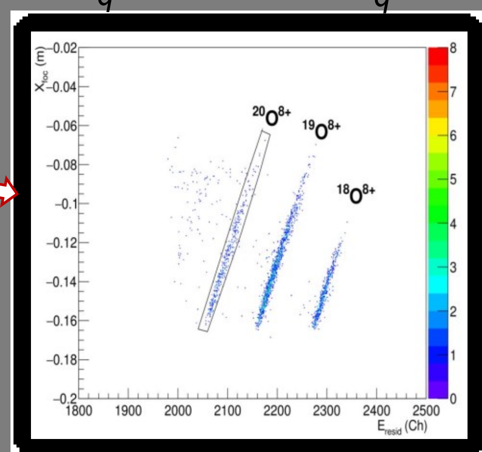

RA RECONSTRUCTION TECHNIQUE

De[redacted]er

ion trajectory

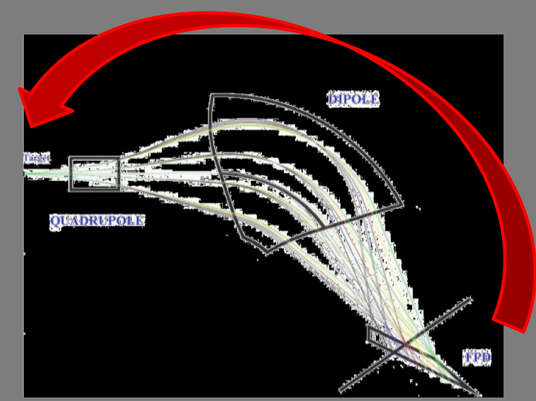

Requires:

- Detailed knowledge of magnetic fields
- Powerful algorithms for solving the transport equations
- High performance detectors

Assures:

- ❖ Good compensation of aberrations
- ❖ Excellent quality of reconstructed parameters

The CS facility

- The CS accelerator current (from 100 W to 5-10 kW);
- The beam transport line transmission efficiency to nearly 100%

From electrostatic extraction
to
Extraction by stripping

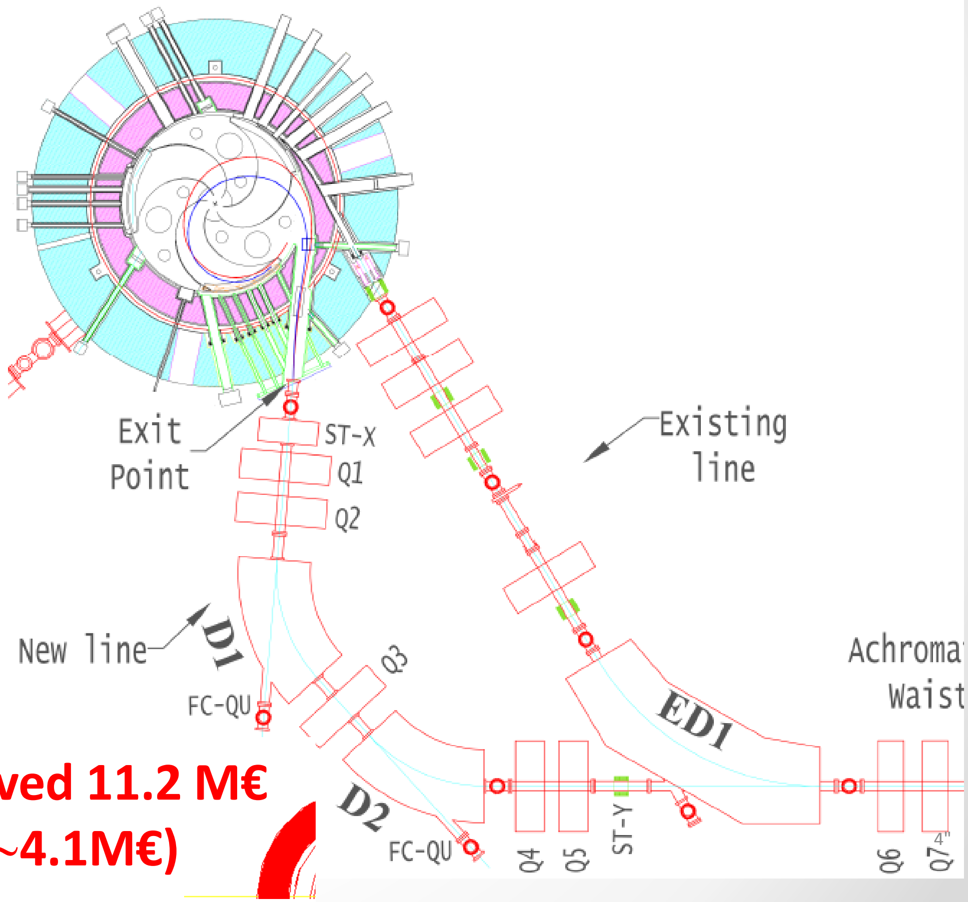

TDR of the project approved 11.2 M€
Cryostat tender started (~4.1M€)

The role of Nuclear Physics

Physics observable

Phase space factor

0νββ decay **half-life**

$$1/T^{0\nu}_{1/2}(0^+ \rightarrow 0^+) = G_{01}\left|M^{\beta\beta 0\nu}\right|^2\left|\frac{\langle m_\nu\rangle}{m_e}\right|^2$$

$$\langle m_\nu\rangle = \sum_i \left|U_{ei}\right|^2 m_i e^{i\alpha_i}$$

new physics inside !

$$\left|M_\varepsilon^{\beta\beta 0\nu}\right|^2 = \left|\left\langle 0_f \left\| \hat{O}_\varepsilon^{\beta\beta 0\nu} \right\| 0_i \right\rangle\right|^2$$

The (^{20}Ne, ^{20}O) reaction

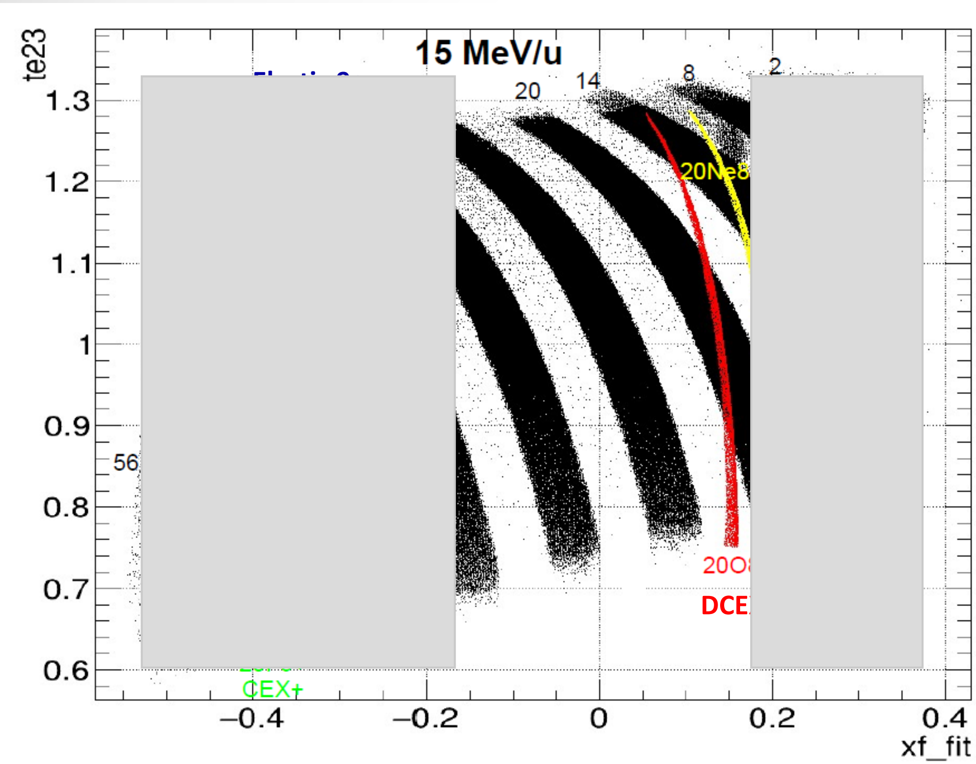

$^{20}Ne^{10+}$ beam passing through the target produces 9^+ and 8^+ charge states

The **$^{20}Ne^{9+}$** has the same magnetic rigidity of **$^{20}F^{9+}$**

The **$^{20}Ne^{8+}$** has the same magnetic rigidity of **$^{20}O^{8+}$**

The use of a post-stripper reduces the amount of 9^+ and 8^+ charge states

NUMEN selected "hot-cases"

Candidates for $0\nu\beta\beta$ already at our reach in terms of energy resolution and availability of thin targets.

^{116}Sn (^{18}O,^{18}Ne) ^{116}Cd – first excited state 513 MeV

^{116}Cd (^{20}Ne,^{20}O) ^{116}Sn - first excited state 1.29 keV

^{76}Ge (^{20}Ne,^{20}°) ^{76}Se - first excited state 562 keV

^{76}Se (^{18}O,^{18}Ne) ^{76}Ge - first excited state 559 keV

^{130}Te (^{20}Ne,^{20}°)^{130}Xe - first excited state …

NME: 2νββ vs 0νββ

NME 2νββ - decay

$$1/T_{1/2}^{2\nu}(0^+ \rightarrow 0^+) = G_{2\nu}\left|M^{\beta\beta 2\nu}\right|^2$$

q-transfer like ordinary β-decay
(q ~ 0.01 fm^{-1} ~ 2 MeV/c)
only allowed decays possible

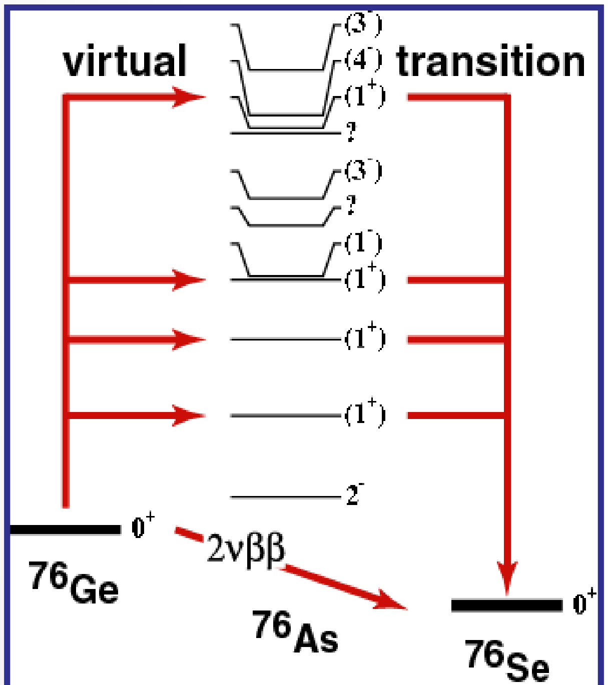

NME 0νββ - decay

$$1/T_{1/2}^{0\nu}(0^+ \rightarrow 0^+) = G_{0\nu}\left|M^{\beta\beta 0\nu}\right|^2\left|\frac{\langle m_\nu\rangle}{m_e}\right|^2$$

neutrino enters as virtual particle,
q~0.5fm^{-1} (~ 100 MeV/c)
degree of forbiddeness weakened

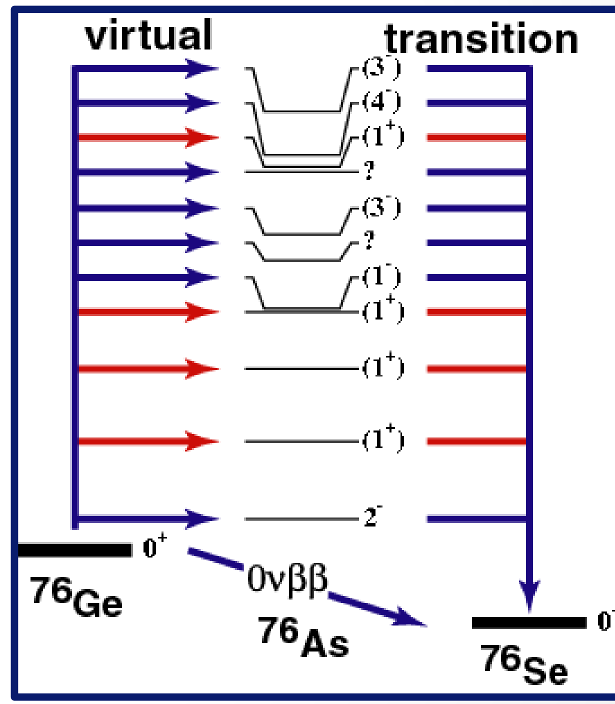

NOT (easily) accessible via charge-exchange reactions

- **Single state dominance**

$$G = \sum_n \frac{|n\rangle\langle n|}{E_n - (E_i + E_f)/2}$$

- **Closure approximation**

DCE cross-section factorization

generalization to DCE:

In analogy to the single charge-exchange, the dependence of the cross-section from q is represented by a Bessel function.

$$\frac{d\sigma^{DCE}}{d\Omega}(q,\omega) = \hat{\sigma}_{\alpha}^{DCE}(E_p, A) F_{\alpha}^{DCE}(q,\omega) B_T^{DCE}(\alpha) B_P^{DCE}(\alpha)$$

unit cross-section

$$\hat{\sigma}_{\alpha}^{DCE}(E_p, A) = K(E_p, 0)|J_{\alpha}^{DCE}|^2 N_{\alpha}^{D}$$

A wide range of DCE cross sections has never been accurately measured due to :

- The difficult to perform **zero degrees** measurements.
- The poor yields in the measured energy spectra and angular distributions, **due to the very low cross sections.**
- **The difficulty to disentangle** possible contributions of **multi-nucleon transfer reactions** leading to the same final state.

MAGNEX Focal Plane Detector

- Gas-filled hybrid detector

Drift chamber 1400mm x200mmx100mm
Pure isobutane pressure range: 5-100mbar; 600-800 Volt,wires 20 micron

Schematic view of the MAGNEX Focal Plane Detector: a) side view; b) top view.

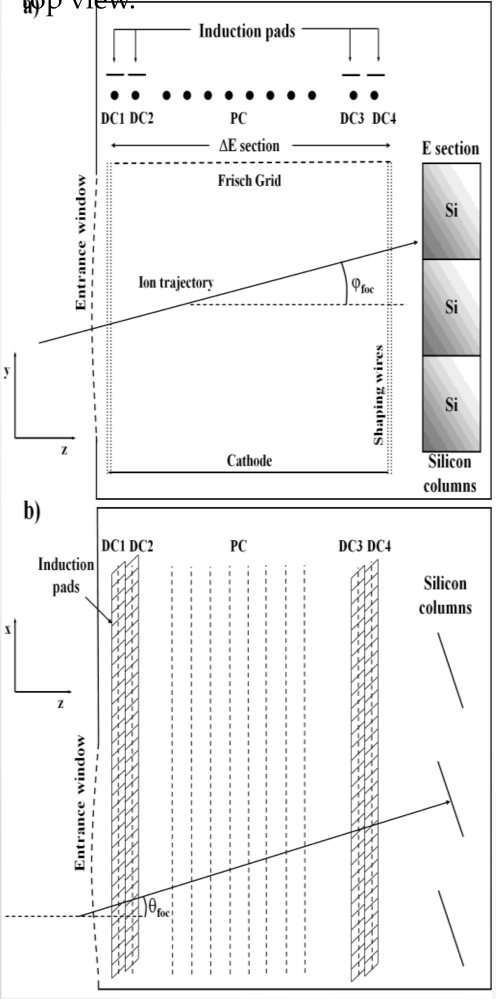

60 Silicon Detectors $\rightarrow E_{res}$

5 Proportional Wires $\rightarrow \Delta E$

Ion identification

4 Induction Strip $\rightarrow X_1, X_2, X_3, X_4 \rightarrow X_{foc}, \theta_{foc}$

4 Drift Chamber (DC) $\rightarrow Y_1, Y_2, Y_3, Y_4 \rightarrow Y_{foc}, \phi_{foc}$

Ray-reconstruction

- Wall Si 500 µm

20 columns, 3 rows

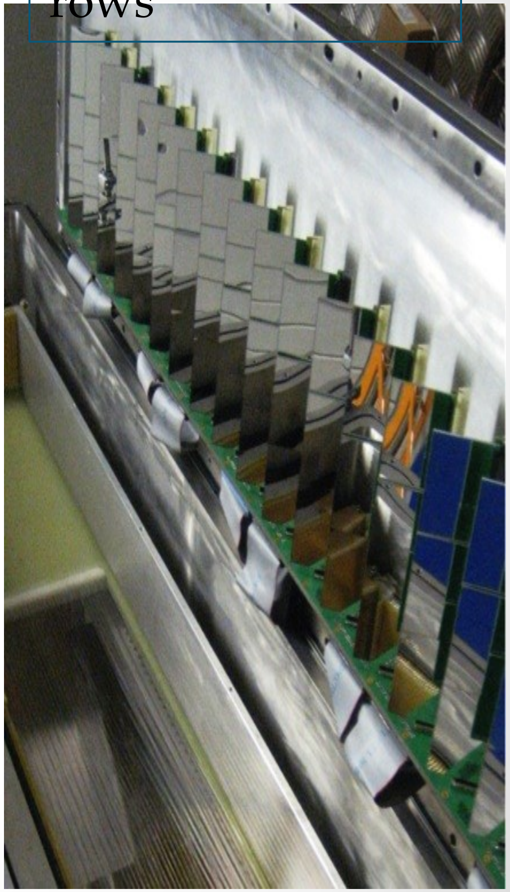

INFN Istituto Nazionale di Fisica Nucleare LNS

Particle identification

Z identification

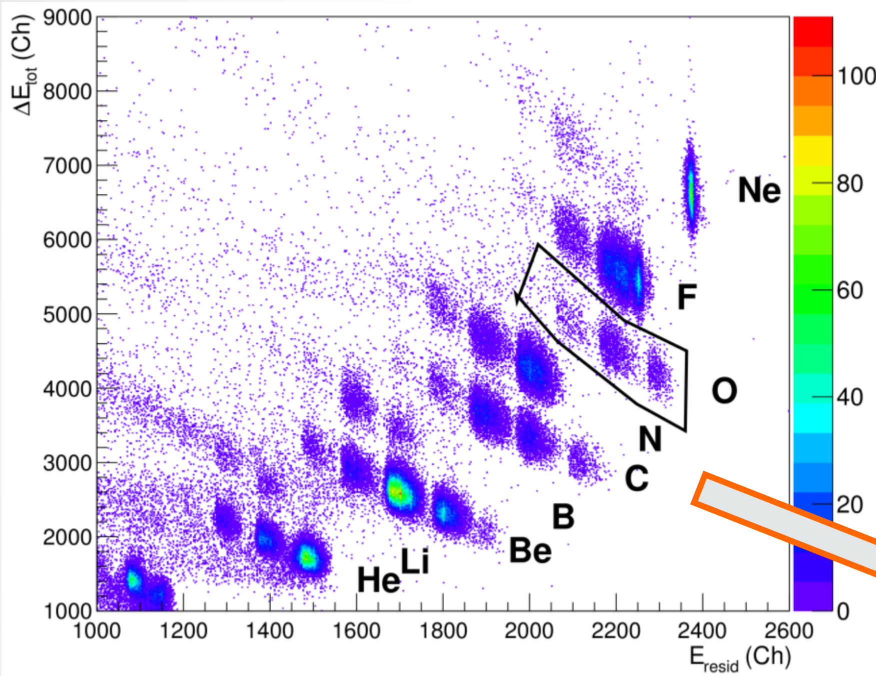

A identification

$$B\rho = \frac{p}{q} \rightarrow X_{foc}^2 \propto \frac{m}{q^2} E_{resid}$$

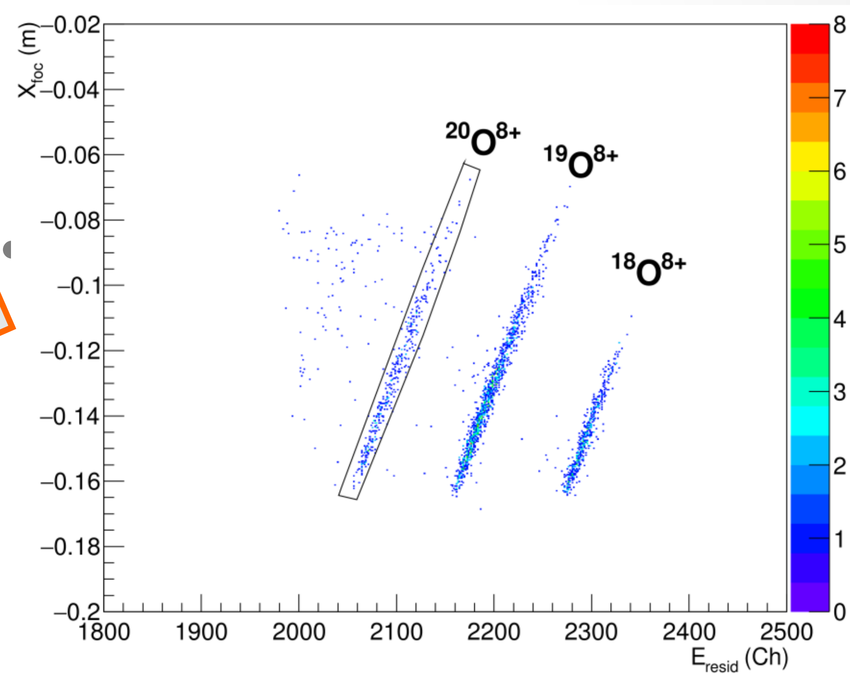

F. Cappuzzello et al., NIMA 621 (2010) 419

The volume integrals

Nuclear spin and isospin excitations

Franz Osterfeld

Reviews of Modern Physics, Vol. 64, No. 2, April 1992

- Volume integrals are **larger at smaller energies**
- They enter to the **fourth power** in the unit cross section!
- **GT-like % F-like competion** at low energy

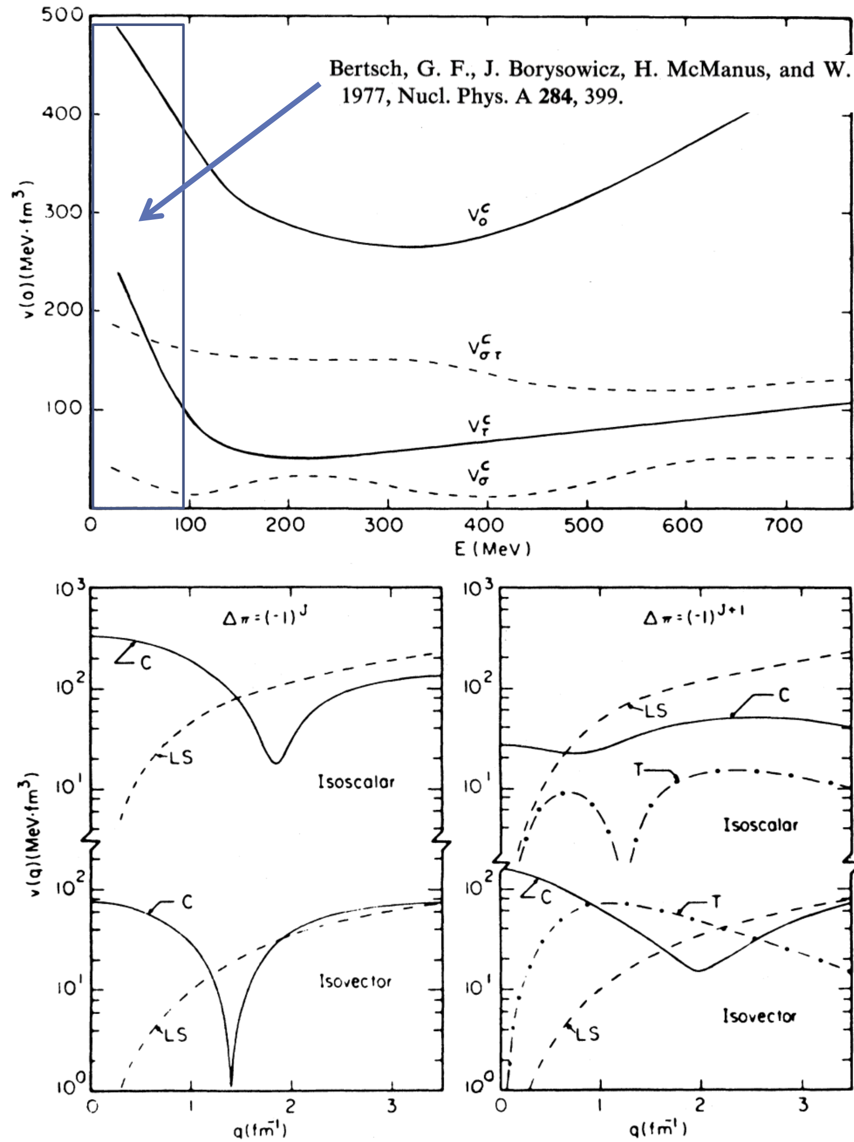

FIG. 15. Energy and momentum dependence of the free nucleon-nucleon t_F matrix. The upper part of the figure shows the energy dependence of the central components of the effective t_F matrix at zero-momentum transfer (including direct and exchange terms). The *G*-matrix interaction of Bertsch *et al.* (1977) was used below 100 MeV and joined smoothly to the t_F matrix above 100 MeV. The lower figures show the momentum dependence of the 135-MeV t_F matrix for natural-(left figure) and unnatural-(right figure) parity transitions. Isoscalar and isovector central (*C*), spin-orbit (*LS*), and tensor (*T*) components are shown. From Petrovich and Love (1981).

Factorization of the charge exchange cross-section

NUMEN

INFN LNS Istituto Nazionale di Fisica Nucleare

for single CEX:

α= Fermi (F)
or Gamow Teller (GT)

$$B(\alpha) = \frac{1}{2J_i+1}|M(\alpha)|^2$$

β-decay transition strengths (reduced matrix elements)

$$\frac{d\sigma}{d\Omega}(q,\omega) = \hat{\sigma}_\alpha(E_p,A)F_\alpha(q,\omega)B_T(\alpha)B_P(\alpha)$$

C.J Guess,et al, PRC 83 064318 (2011)

unit cross-section

$$\hat{\sigma}(E_p,A) = K(E_p,0)|J_\alpha|^2 N_\alpha^D$$

T.N.Taddeucci, et al, Nucl. Phys. A 469 (1987) 125

The factor $F_\alpha(q,\omega)$ describes the shape of the cross-section distribution as a function of the linear momentum transfer and the excitation energy.

(d,^{2}He)

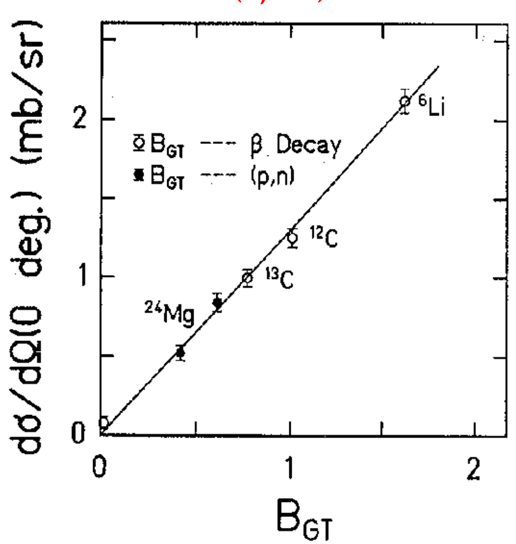

Fig. 12. The measured cm cross-sections of the (d,^{2}He) reactions at 0° as a function of the G' strengths deduced from β-decay or (p,n) reaction studies. The solid line is a linear "t to the data [244].

Y. Fujita Prog. Part. Nuc. Phys. 66 (2011) 549
F. Osterfeld Rev. Mod. Phys. 64 (1992) 491
H. Ejiri Phys. Rep. 338 (2000) 256
T.N. Taddeucci Nucl. Phys. A 469 (1997) 125

(^{7}Li,^{7}Be) S. Nakayama PRC 60 (1999) 047303

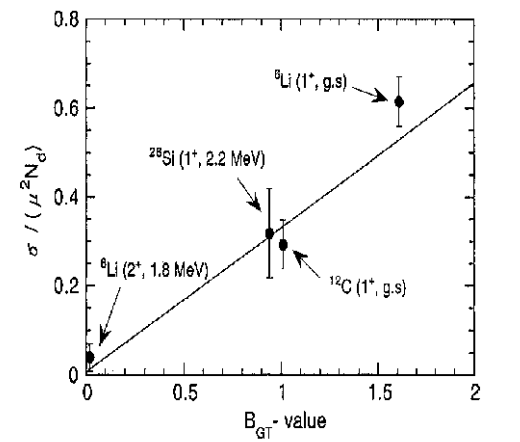

Fig. 18. Cross-sections σ/(μN^2) for G' transitions in the (^{7}Li,^{7}Be) reactions at 0° and B(G') values. μ and N^2 are the reduced mass and the distortion factor, respectively [197].

B(GT;CEX)/B(GT;β-decay) ~ 1 within a few % especially for the strongest transitions